The spatial and inter-annual dynamics of the surface water carbonate system and air-sea CO_2 fluxes in the outer shelf and slope of the Eurasian Arctic Ocean

Irina I. Pipko[1,2], Svetlana P. Pugach[1,2], Igor P. Semiletov[1,2,3], Leif G. Anderson[4], Natalia E. Shakhova[2,3], Örjan Gustafsson[5,6], Irina A. Repina[7], Eduard A. Spivak[1], Alexander N. Charkin[1,2], Anatoly N. Salyuk[1,2], Kseniia P. Shcherbakova[1,2], Elena V. Panova[2], Oleg V. Dudarev[1,2]

[1]V.I. Il'ichev Pacific Oceanological Institute, Russian Academy of Sciences, Vladivostok, 690041, Russia
[2]National Research Tomsk Polytechnic University, Tomsk, 634050, Russia
[3]International Arctic Research Center, University of Alaska Fairbanks, Fairbanks, AK 99775, USA
[4]Department of Marine Sciences, University of Gothenburg, Gothenburg, 412 96, Sweden
[5]Department of Environmental Science and Analytical Chemistry, Stockholm University, Stockholm, 10691, Sweden
[6]Bolin Centre for Climate Research, Stockholm University, Stockholm, 10691, Sweden
[7]A.M. Obukhov Institute of Atmospheric Physics, Russian Academy of Sciences, Moscow, 119017, Russia

Correspondence to: Irina I. Pipko (irina@poi.dvo.ru)

Abstract. The Arctic is undergoing dramatic changes which cover the entire range of natural processes, from extreme increases in the temperatures of air, soil, and water, to changes in the cryosphere, the biodiversity of Arctic waters, and land vegetation. Small changes in the largest marine carbon pool, the dissolved inorganic carbon pool, can have profound impact on the carbon dioxide (CO_2) flux between the ocean and the atmosphere, and the feedback of this flux to climate. Knowledge of relevant processes in the Arctic seas improves the evaluation and projection of carbon cycle dynamics under current conditions of rapid climate change.

Investigation of the CO_2 system in the outer shelf and continental slope waters of the Eurasian Arctic seas (the Barents, Kara, Laptev, and East Siberian seas) during 2006, 2007, and 2009 revealed a general trend in the surface water partial pressure of CO_2 (pCO_2) distribution, which manifested as an increase in pCO_2 values eastward. The existence of this trend was defined by different oceanographic and biogeochemical regimes in the western and eastern parts of the study area; the trend is likely increasing due to a combination of factors determined by contemporary change in the Arctic climate, each change in turn evoking a series of synergistic effects. A high-resolution in situ investigation of the carbonate system parameters of the four Arctic seas was carried out in the warm season of 2007; 2007 was characterized by the next-to-lowest historic sea ice extent in the Arctic Ocean, on satellite record, to that date. The study showed the different responses of the seawater carbonate system to the environment changes in the western vs. the eastern Eurasian Arctic seas. The large open, highly productive water area in the northern Barents Sea enhances atmospheric CO_2 uptake. In contrast, the uptake of CO_2 was strongly weakened in the outer shelf and slope waters of the East Siberian Arctic seas under the 2007 environmental conditions. The surface seawater appears in equilibrium or slightly supersaturated by CO_2 relative to atmosphere because of the increasing influence of river

runoff and its input of terrestrial organic matter that mineralizes, in combination with the high surface water temperature during sea ice-free conditions.

This investigation shows the importance of processes that vary on small scales, both in time and space, for estimating the air-sea exchange of CO_2. It stresses the need for high-resolution coverage of ocean observations as well as time series. Furthermore, time series must include multi-year studies in the dynamic regions of the Arctic Ocean during these times of environmental change.

1 Introduction

The Arctic is currently undergoing dramatic changes which cover the entire range of natural processes; from extreme increases in the temperatures of air, soil, and water, to changes in the biodiversity of Arctic waters and land vegetation (Serreze and Barry, 2011; Bhatt et al., 2010). In 1896, the Swedish scientist Svante Arrhenius hypothesized that changes in the atmospheric concentration of carbon dioxide (CO_2) could alter the earth's surface temperature and that this temperature change would be especially large in polar latitudes. This likely is the first formal description of what today is known as the Arctic amplification, i.e., a higher temperature increase in Arctic regions than in other regions of the globe (Serreze and Barry, 2011; Jeffries et al., 2013). The changes being observed today will probably become more intense in the coming decades through positive feedback, causing further changes in atmospheric circulation, river discharge, the carbon cycle, vegetation, conditions of terrestrial and submarine permafrost, and many other natural processes; the consequences will be noticed within, as well as outside of the Arctic region (Serreze and Barry, 2011; Anderson et al., 1998; Macdonald et al., 2008; Semiletov et al., 2000, 2016; Shakhova et al., 2014). Currently, these changes refer to a "new condition" of the Arctic climate (Kattsov et al., 2010; Jeffries et al., 2013; Wood et al., 2015).

The most obvious indicator of Arctic climatic change is the change of sea ice cover, with a persistent decline in areal extent during the last decades. Since the start of satellite observations in 1979 the sea ice extent in March, the period of maximum coverage, has declined by 2.6 % per decade (Serreze et al., 2007; Stroeve et al., 2012; Jeffries et al., 2013). However, during the last decade the September sea ice extent has decreased by 13 % relative to the 1979 – 2000 average (Jeffries et al., 2013). The change in sea ice coverage is most pronounced in the large Eastern Arctic shelf seas (ftp://sidads.colorado.edu). Moreover, the melt season has lengthened by 1-2 weeks per decade, and with continued Arctic warming it will expand further (Stroeve et al., 2014).

The environmental conditions vary between the Eurasian shelf seas, of which the Barents Sea is one of the largest and deepest (Jakobsson, 2002). According to the classification of Carmack et al. (2006), the Barents Sea is considered an "inflow" shelf sea or an Atlantic-influenced shelf sea (Findlay et al., 2015). The general inflow of warm and salty water from the Atlantic keeps a large part of the Barents Sea ice-free all year round. In the northern area a portion of the warm Spitsbergen Current returns around Svalbard to the Barents Sea as "cold Atlantic" water (Kaltin et al., 2002) or "Arctic" water (Loeng, 1991). This area is largely covered with ice, but at a variable extent over the year, and the presence of polynyas contributes to water

salinization in the winter (Carmack et al., 2006). However, the cooling of the Atlantic water (AW) during its passage through the Barents Sea produces the largest volume of high-density water that ventilates the deep Eurasian Basin water (Schauer et al., 2002). The Barents Sea receives little river input compared to other Arctic shelf seas (Anderson et al., 1998; Schauer et al, 2002). Due to high primary productivity (PP) and cooling during transit to the north, the waters of the Barents Sea constitute
70   the strongest all-season sink for atmospheric CO_2 in the Arctic (Fransson et al., 2001; Omar et al., 2007; Bates and Mathis, 2009; Årthun et al., 2012; Lauvset et al., 2013).

The other shelf seas (the Kara, Laptev, and East Siberian seas) are classified as "interior" shelf seas (Carmack et al., 2006) or as river-influenced shelf seas (Findlay et al., 2015). The river discharge as well as the seasonal formation and melting of sea ice greatly impact the hydrology and chemistry of these shelf seas. Water of Atlantic origin enters the Kara Sea from the
75   Barents Sea, and the Kara Sea also receives more than a third of the volume of riverine discharge flowing into the Arctic Ocean, mainly via the Ob and Yenisei rivers.

The shallow East Siberian and Laptev seas, together with the Chukchi Sea, form a large, broad, and shallow province composing as much as 22 % of the entire Arctic Ocean area but only 1 % of the volume (Jakobsson, 2002). The Laptev Sea and the East Siberian Sea are surrounded and underlain by permafrost and are characterized by the degradation of coastal ice-
80   complex and terrestrial permafrost containing an extensive pool of ancient labile organic matter (OM) (Semiletov, 1999; Sánchez-García et al., 2014; Schirrmeister et al., 2011; Tesi et al., 2014; Vonk et al., 2014). They are strongly impacted by the input and transformation of terrestrial OM (Charkin et al., 2015; Dudarev et al., 2006; Gustafsson et al., 2011; Mann et al., 2012, 2015; Semiletov et al., 2007, 2016; Tesi et al., 2016; Bröder et al., 2016; Vonk et al., 2014). The input of suspended as well as dissolved terrigenous material (Alling et al., 2010; Raymond et al., 2007; Holmes et al., 2012) including optically-
85   active fractions of dissolved OM, colored dissolved OM (CDOM; Pugach et al., 2015, 2017), and the presence of ice cover throughout a significant part of the year reduces the depth of solar radiation penetration into the water column. Together with limited nutrient content, these conditions make these seas unproductive, 5-10 times less productive than inflow shelves (Carmack et al., 2006). Moreover, intense inflow of terrigenous OM, low productivity, as well as subsea release of methane that partly oxidizes (Shakhova et al., 2015), make significant areas of these seas heterotrophic, and thus CO_2 sources to the
90   atmosphere (Anderson et al., 2009, 2011; Pipko et al., 2005, 2011a; Semiletov et al., 2007, 2012, 2013).

The waters of the Arctic seas have become warmer and fresher than they were several decades ago (Wood et al., 2015); among other effects, this warming and freshening has caused increased OM input to the shelf seas, resulting in severe aragonite undersaturation (Semiletov et al., 2016). It has been shown that the acidifying effect of terrestrial OM decomposition at an erosion-dominated site was more than five times stronger than that of estuary freshening.
95   How climate change impacts the contemporary carbon cycle in the Eurasian Arctic Seas, including its consequences for transformation and fluxes, has been the subject of intense interest during the last decade (Anderson et al., 2011; Bischoff et al., 2016; Bröder et al., 2016; Charkin et al., 2015; Gustafsson et al., 2011; Karlsson et al., 2016; Macdonald et al., 2008; Sánchez-García et al., 2014; Tesi et al., 2014; Vonk et al., 2014). Small changes in the largest marine carbon pool, the dissolved inorganic carbon (DIC) pool, can have profound impacts on the CO_2 flux between the ocean and the atmosphere and the

feedback of this flux to climate. Knowledge of relevant processes in the Arctic seas improves the evaluation and projection of carbon cycle dynamics under conditions of rapid climate change. The East Siberian Arctic seas (ESAS), including the Laptev Sea, the East Siberian Sea, and the Russian sector of the Chukchi Sea, are especially relevant in this perspective because they have the broadest and the shallowest shelves among the Arctic seas, they receive large volumes of river discharge, they are characterized by high rates of coastal erosion, and their drainage basins are underlain by permafrost (Macdonald et al., 2008; Semiletov et al., 2000, 2012).

Studies of the Barents Sea carbonate system (Årthun et al., 2012; Lauvset et al., 2013; Pipko et al., 2011b; Yakushev and Sørensen, 2013) as well as the ESAS waters (Anderson et al., 2009, 2011; Pipko et al., 2011a, 2015, 2016; Semiletov et al., 2012, 2013, 2016) have been performed during the last decade. The Kara Sea remains less studied in the context of carbonate system dynamics and the main research was accomplished in the shallow part of this sea (Makkaveev et al., 2010, 2015). Most of the ESAS studies were carried out in ice-free areas, i.e. at depths normally limited to 70 m isobaths, which corresponds to the area of the inner and middle shelves. Meanwhile, the deep part of the seas where the changes in the ice cover are most pronounced is the least investigated. To date, only one paper dedicated to CO_2 system dynamics in the East Siberian Sea outer shelf is available (Anderson et al., 2017); it is based on the field campaign accomplished within the framework of the SWERUS-C3 (Swedish - Russian - US Arctic Ocean Investigation of Climate - Cryosphere - Carbon Interactions) program aboard the Swedish icebreaker *Oden*. This study was accomplished in ice conditions, with the sea ice concentration ranging between 70 and 100 %.

The objective of this contribution is to evaluate the importance of the meteorological and oceanographic conditions and biogeochemical processes which determine the surface water partial pressure of CO_2 (pCO_2) and air-sea CO_2 fluxes in the outer regions of the Eurasian Arctic seas' shelf/slope system along the AW inflow path in different years. This will add to the knowledge of the regional sensitivity to current changes and thus project the response of the entire Arctic carbon cycle to global climate warming.

2 Materials and methods

2.1 Study area

The study is based on observational data collected in the Eurasian sector of the Arctic Ocean during the summer-fall (late August-early October) seasons of 2006, 2007, and 2009 (Fig. 1). An extensive investigation of the outer shelf and continental slope of the Barents, Kara, and Laptev seas and the northwestern East Siberian Sea was performed during the 2007 expedition on the research vessel *Viktor Buynistkiy* within the framework of the Nansen and Amundsen Basins Observational System (NABOS) program (Fig. 1). Data collected in 2006 and 2009 within the framework of the NABOS program on board the icebreaker *Kapitan Dranitsyn* were used for comparative analysis (Fig. 1).

2.2 Methods

2.2.1 Hydrological data

During all cruises, water samples for chemical analysis were taken with a standard Rosette system equipped with the SBE19+ CTD (conductivity, temperature, depth) probe to record conductivity and temperature. In 2007 another SBE19+ probe equipped with the same sensors was deployed in a 150 L plastic barrel into which flowing seawater was pumped from the depth of about 4 m at the rate of about 80 liters per minute.

2.2.2 Total alkalinity (A_T)

Water samples were poisoned with a mercuric chloride solution at the time of sampling to halt biological activity (Dickson et al., 2007) and were stored in the dark at room temperature until they were analyzed ashore. Samples for A_T were analyzed in the lab within one month using an indicator titration method in which 25 ml of seawater was titrated with 0.02 M HCl in an open cell according to Bruevich (1944) and Pavlova et al. (2008). Measurements were performed at 20 °C, with the temperature in the cell controlled to within 0.1 °C. In 2000 the Carbon Dioxide in the Ocean working group of the North Pacific Marine Science Organization (PICES) performed an intercalibration of A_T in seawater using certified reference materials (CRMs). The results of the intercalibration showed that the alkalinity values obtained by the Bruevich method are in agreement with the standard within ±1 µmol kg^{-1} when state-of-the-art analytical practice is applied (Pavlova et al., 2008). A_T measurements were performed with a precision of ~2 µmol kg^{-1} with the accuracy set by calibration against CRMs supplied by A. Dickson, Scripps Institution of Oceanography (USA). Batch #96 was used in 2009. In the 2006 and 2007 cruises the HCl concentration was determined using a standard solution of Na_2CO_3 made up by carefully weighing Na_2CO_3 of 99.995 % purity (DOE, 1994; Pavlova et al., 2008).

2.2.3 pH

A potentiometric method was applied to determine pH on the Pitzer pH scale (Pitzer, 1991) using a closed cell held at constant 20 °C temperature with a sodium and hydrogen glass electrode pair without liquid junctions (Tishchenko et al., 2001, 2011). A TRIS–TRIS–HCl–NaCl–H_2O buffer solution (Tishchenko, 2000, 2011) was used for calibrations on the Pitzer pH scale. Both the hydrogen glass electrode and the sodium glass electrode were calibrated using this buffer. Together with thermodynamic data (Dickson, 1990a) the pH values were converted from the Pitzer pH scale to the total hydrogen ion concentration scale (pH_T20) (Tishchenko et al., 2001, 2011; Dickson et al., 2007). The precision of pH measurements was about 0.004 pH units, with the accuracy set by calibration against buffer solution on the Pitzer pH scale.

2.2.4 Partial pressure of CO_2

Continuous measurements of pCO_2 were performed in the surface mixed layer using a Submersible Autonomous Moored Instrument for CO_2 (SAMI-CO_2) Sensor with a precision of ±1 µatm (DeGrandpre et al., 1995). The sensor was deployed in the same barrel as the SBE19+ probe. The calibration procedures are described in detail in DeGrandpre et al. (1995). The

temperature in the barrel was 0.55 °C higher than the sea-surface temperature and the pCO_2 measurements were corrected to in situ temperature using the equation of Takahashi et al. (1993). All in situ surface data described in this paper were averaged over 15 minute intervals.

At oceanographic stations surface pCO_2 values were calculated, on discrete samples, from pH_T20, A_T, and inorganic nutrients data using the CO2SYS program of Lewis and Wallace (1998) with equilibrium constants of Mehrbach et al. (1973) refit by Dickson and Millero (1987), using the sulfate and borate dissociation constants of Dickson (1990a, b).

2.2.5 Wind speed

The wind speed was measured using an automated meteorological station (Gradient Automatic Weather Station AWS2700) located at a height of 15-20 m above sea level. The true wind speed was calculated using navigation information and was extrapolated to the height of 10 m.

2.2.6 CO$_2$ flux calculation

Air-sea CO_2 fluxes were calculated using the diffusive boundary layer model:

$$F = K_w \, S \, \Delta pCO_2 \, (1\text{-}f_{ice}), \tag{1}$$

where F is gas flux (e.g. in mmol CO_2 m^{-2} day^{-1}), K_w is gas-transfer velocity, S is CO_2 solubility (Weiss, 1974), ΔpCO_2 is the difference between the atmospheric and oceanic pCO_2, and f_{ice} is the fraction of sea ice coverage. Two relationships were used for calculating gas-transfer velocity (Wanninkhof, 1992 and Wanninkhof and MacGillis, 1999). Gas-transfer velocities were calculated using onboard measured wind speed.

2.2.7 Apportionment of freshwater (FW) fractions

In order to determine the composition of water samples, we used a three-component mass balance, using salinity and A_T in this evaluation (e.g. Ekwurzel et al., 2001; Fransson et al., 2001, 2009). The major FW sources are river water (RW) and sea ice meltwater (MW), both mainly originating from the Arctic shelf areas. It is assumed that each summer sample is a mixture of Atlantic-derived seawater (SW; f_{SW}), RW (f_{RW}), and sea ice MW (f_{MW}). For riverine A_T, the average value of 840 μmol kg^{-1} was applied, which is typical of the largest Siberian rivers (the Ob, Yenisei, and Lena rivers) during the warm season (Tank et al., 2012); up to 90 % of the total river discharge enters the Arctic Seas during this season (Dittmar and Kattner, 2003). The sea ice values of salinity and A_T are taken from Fransson et al. (2009); the Atlantic-derived water values of salinity and A_T are taken from Pipko et al. (2011b).

This gives us the following equations for computing the mass balance:

$$1 = f_{SW} + f_{RW} + f_{MW}; \tag{2}$$

$$S = 34.90 \, f_{SW} + 5 \, f_{MW}; \tag{3}$$

190      $A_T = 2292\ f_{SW} + 840\ f_{RW} + 349\ f_{MW}.$ (4)

2.2.8 Statistical treatment and graphical representation of the data

Data were tested statistically using an empirical distribution function test in the Statistics 7.0 software package. Descriptive statistics were calculated for the 95 % confidence interval of the mean (P=0.95, alpha=0.05). Most of the plots and maps in this study were created with the Ocean Data View software (Schlitzer, 2011).

195   ## 3 Results and Discussion

3.1 Meteorological conditions

In the summer season of 2006, low sea level pressure (SLP) dominated over the Arctic Ocean (Fig. 2a), resulting in dominating westerly winds that hampered penetration of RW into the central Arctic Ocean, as well as northern to northwestern sea ice drift. The area of sea ice cover was maximal (5.9 million km^2) and the sea ice edge in 2006 had the most southern position of

200   the three years studied (Fig. 1a), which also impeded the transfer of surface water to the deeper part of the ocean. The negative sea ice concentration anomaly was strongest to the east of the study area, while the total anomaly for the whole Arctic Ocean was -0.5 million km^2 compared to the mean coverage during the 1981-2010 time period (ftp://sidads.colorado.edu). The sea ice conditions varied from light to ice free in the central Laptev Sea to heavy north of the Novaya Zemlya islands where the concentration reached 90-100 %.

205   The Arctic Dipole (AD), which is characterized by low SLP on the Eurasian side of the Arctic and high SLP on the American side, was present *in the summer of 2007* (Fig. 2b) and contributed to a 2007 record minimum sea ice extent (Overland et al., 2014). The AD pattern persisted for part of the summer during each year following 2007. The interplay between the two regional centers of atmospheric pressure controlled the wind pattern, especially over the ESAS. The maximum summer winds and the most intensive transfer of RW and sea ice to the north and northwest occurred in the warm season of 2007, forced by

210   the extreme pressure gradient between the two centers of action (Fig. 2b). In fact, strong winds were experienced during the 2007 cruise, with wind speed reaching 22 m sec^{-1} in the western study area and 13 m sec^{-1} in the eastern. In 2007 the sea ice anomaly reached -1.6 million km^2 for the entire Arctic Ocean. The negative anomaly in the sea ice concentration shows how much the ice concentration for a particular month in one year differs from the mean calculated for that month from 1981 to 2010; that mean was maximal in the ESAS, exceeding 50 % (ftp://sidads.colorado.edu). Actually, the entire study region was

215   largely ice-free in 2007.

A high-pressure area was also present over the American side of the Arctic Ocean *in the summer of 2009*, with comparable pressure in the center of the anticyclone but with an even larger extent than in 2007 (Fig. 2c). However, the low-pressure center over the Siberian Arctic was much weaker, resulting in a weaker SLP gradient and correspondingly weaker wind. A significant part of the study area was covered with ice in 2009, with the sea ice concentration reaching 95-100 % (Fig. 1). The total Arctic

220   Ocean anomaly of sea ice concentration in 2009 was also negative at -1.0 million km^2 (ftp://sidads.colorado.edu). Maximal

interannual deviations in the sea ice extent were detected in the ESAS, while the position of the sea ice edge in the Barents Sea was far to the north and did not differ much between the years (Fig. 1a).

3.2 Oceanographic observations

3.2.1 Temperature

In 2006, the temperature was close to the freezing point in the regions where sea ice was present, in the northern Barents and Kara seas as well as in the deep basin north of the Laptev Sea; surface temperatures varied from -1.82 to 3.30 °C. The highest temperatures (maximum 3.90 °C) were found in the ice-free waters of the Laptev Sea (Fig. 3). *In 2007*, low sea surface temperatures were found in the northern Barents Sea east of Svalbard, in the northern Kara Sea, and in Vilkitsky Strait (down to -1.13 °C, Fig. 4). These low temperatures were associated with the ice edge vicinity and the presence of sea ice in Vilkitsky Strait (Fig. 1). The waters in the northwestern Barents Sea retained the original AW characteristics ($2 < T < 5$ °C and $S > 34.8$, Hopkins, 1991). The highest sea surface temperatures (up to 4.11 °C) were measured west and north of Svalbard (Fig. 4). High surface water temperatures were also measured in the Laptev Sea (~ 3.70 °C) and over the Lomonosov Ridge (Fig. 4). *In 2009*, surface water temperatures varied from -1.73 to 2.85 °C (Fig. 5). Temperature remained < 0 °C over most of the study area with > 0 °C values in the ice-free areas of the Laptev Sea and the Kara Sea.

3.2.2 Salinity

In 2006, the sea surface salinity, as measured at the oceanographic stations, covered a range from 27.00 to 33.57 (Fig. 3). High salinity was observed along the AW inflow path, i.e. in the northern Barents and Kara seas. As it enters the northern Laptev Sea the water's salinity decreases through mixing with river runoff; the lowest salinity was measured in the ice-free waters of the Laptev Sea (Fig. 3). The sea surface salinity within the study region *in 2007* varied substantially, as was expected considering the differences in oceanographic regimes of the studied seas. In the West Spitsbergen Current, the AW salinity was close to 35; it slowly decreased along the cruise track in the northwestern Barents Sea, slightly varied in the central part of the sea, and decreased in the eastern part (Fig. 4). In the eastern Kara Sea, which is influenced by river runoff, the salinity decreased to well below 30, a salinity level that also was observed in the western Laptev Sea as well as at the Laptev Sea continental slope. The lowest salinities were observed in the eastern Laptev Sea and northwestern East Siberian Sea, reaching well below 25 (Fig. 4). *In 2009*, the surface water salinity varied from 28.79 to 33.88 with relatively constant salinity in the waters of the Barents and the Kara seas, while it dropped sharply when entering the Laptev Sea where the lowest values were observed (Fig. 5).

3.3 Surface water pCO$_2$ spatial distribution in 2007

Seawater pCO$_2$ is affected by several processes. Some are physical, such as temperature and vertical as well as horizontal advection; others are biological, such as production/mineralization of OM. The importance of these processes for the surface

pCO_2 values observed in fall 2007, which was characterized by the next-to-lowest historic sea ice extent in the Arctic Ocean to that date, is discussed in the following.

3.3.1 The Barents Sea

The Barents Sea is an inflow shelf where the supply of nutrients from the Atlantic forms the basis for high PP. This, together with the accompanying heat loss, results in year-round CO_2 undersaturation of the surface layer. Consequently it is an annual sink for atmospheric CO_2, though with large spatial variability (Fransson et al., 2001; Kaltin et al., 2002; Nakaoka et al., 2006; Omar et al., 2007; Bates and Mathis, 2009; Lauvset et al., 2013). Of the Arctic shelf seas, the Barents Sea can only compare with the highly productive Chukchi Sea where the surface pCO_2 can drop down to 100 µatm during the warm productive season (Bates, 2006; Pipko et al., 2002).

Our investigation shows that the surface waters in the less-studied northern Barents Sea were also undersaturated and thus the northern Barents Sea is a sink of atmospheric CO_2 (Fig. 4). The waters to the west of Svalbard are undersaturated by about 50 µatm, which is typical for this region when the flux from the atmosphere cannot keep up with the decrease in pCO_2 caused by the cooling of the northward-flowing water. During its flow to the north/northeast the surface water is cooled further, mainly by melting sea ice; thus, it also freshens. Therefore, the temperature of surface waters decreased by ~4.5 °C (from ~4 °C to ~-0.5 °C, Fig. 4) at 9-24° E longitude; this caused a thermodynamic decrease of pCO_2, calculated according Takahashi et al. (1993), by ~70 µatm. The correlation between temperature and pCO_2 in this region was strong (R = 0.84), further emphasizing the importance of temperature in determining pCO_2 here (Fig. 6). An additional pCO_2 decline resulted from the addition of sea ice MW, normally undersaturated in CO_2 (Nedashkovsky and Shvetsova, 2010; Rysgaard et al., 2012); the calculated sea ice MW fraction was up to 10 % in the northeastern Barents Sea (Fig. 7). PP could have also contributed to lowering pCO_2 even if this study had occurred at the end of the productive season (end of September – beginning of October) because air – sea exchange might not have compensated fully for the biological drawdown.

To the east, in the northern Barents Sea, surface temperatures varied slightly with longitude and remained negative; salinity slowly decreased from 24-53° E longitude, and then reduced to ~ 31 near 65° E longitude (Fig. 6). In the eastern Barents Sea, the relationship between pCO_2 values and temperature was weak; salinity demonstrated a significant spatial variability, but a pCO_2-salinity correlation was practically absent (Fig. 6). Therefore, in the northern Barents Sea, pCO_2 variability is driven by different processes in northeastern and northwestern parts of the sea; the temperature impact predominates in the west, and the influence of MW predominates eastward.

3.3.2 The Kara Sea

The Kara Sea surface waters were undersaturated in pCO_2 with the lowest values in the west and highest to the east (Fig. 4). The pCO_2 correlation with temperature was weak (R = 0.28) for the entire Kara Sea, but pCO_2 was strongly negatively correlated with salinity (R = -0.72). Generally, the Kara Sea has two oceanographic sub-regions with different regimes, the

western part where Atlantic origin water dominates, slightly modified by sea ice melt, and the *eastern part* where this modified water is further diluted by river runoff from two Great Siberian rivers, the Ob and the Yenisei. This pattern is set by the general eastward direction of water transport in the Eurasian Arctic seas (e.g., Olsson and Anderson, 1997), but wind is the main driving force of the north RW flow in the Kara Sea (Harms and Karcher, 1999). In early summer 2007, with intensive AD development (Fig. 2), a western RW transport developed; in late summer a northern/northeastern type of RW distribution predominated (Zatsepin et al., 2010) and the deep part of the sea was partly influenced by these waters. Note that in 2007 the discharge of the Ob and Yenisei rivers was the largest of the three years studied (2006, 2007, and 2009) and exceeded (+23 % and +4 %, respectively) the average multi-year value for the 1999-2009 period (426 and 663 km³, respectively) (PARTNERS and ArcticGRO Projects data); this river discharge additionally affected the northeastern Kara Sea.

Hence, we examine separately the relationships of pCO_2 with the hydrographic characteristics of the western and eastern regions (Fig. 8). The lack of reliable correlation of pCO_2 with the hydrography in the western Kara Sea was analogous to the northeastern Barents Sea. This emphasizes the fact that a similar source of water as well as similar processes that determine the carbonate system dynamics occurred in this part of the Eurasian Arctic seas; sea surface temperature slightly changed and MW was the predominant source of FW.

In contrast, processes determining carbonate system dynamics in the eastern Kara Sea were clearly different. The examination revealed a high positive correlation between pCO_2 and temperature (R = 0.84) and a strong negative correlation of pCO_2 with salinity (R = -0.62) in the eastern part of the sea (Fig. 8). Together with the increase of pCO_2 toward the east, significant correlations of pCO_2 values with hydrological parameters pointed to the role of RW. Riverine discharge added to the seawater warming, increased the pCO_2, and contributed water enriched with CO_2; pCO_2 was also increased via decay of terrestrial OM, transported with RW.

The negative correlation found in the eastern Kara Sea is typical for regions influenced by warm RW, with high pCO_2 and labile OM as a substrate for further CO_2 production (Semiletov et al., 2013). Furthermore, together with salinity, pCO_2 is a useful tracer of the river plume distribution within the Kara Sea (Fig. 8).

Note that, despite the presence of RW in the eastern part of the sea, the surface pCO_2 values remained below atmospheric values.

3.3.3 The Laptev Sea

High pCO_2 was observed in the Laptev Sea surface waters, even to levels that exceeded atmospheric (Fig. 4). Supersaturation was observed in the southern Laptev Sea outside the Lena River Delta, which is typical in surface waters of the eastern Laptev Sea inner and middle shelves (Anderson et al., 2009; Semiletov et al., 2012, 2013; Pipko et al., 2016). Moreover, high pCO_2 was also observed in the surface waters of the outer Laptev Sea shelf over the Lomonosov Ridge and further to the east (Fig. 4). The computed RW fraction reached 30-35 % in the southern Laptev Sea and decreased to 5-7 % north of the latitudinal transect extending from the Lena Delta (Fig. 7). High RW content in the surface water (up to 33 %) was also found over the Lomonosov Ridge, which indicated a more efficient northeastern transport of RW in the ice-free conditions of 2007. Thus,

under intensive AD development the northeastern transfer of RW prevailed and maximal RW content was found in the surface slope water over the Lomonosov Ridge. The MW played a small role on the middle and outer shelves; a strong sea-ice-related brine signal was found here (the brine fraction reached 10 %). In the western outer shelf of the Laptev Sea the surface waters were undersaturated in CO_2 relative to atmosphere; the lowest values were observed furthest to the north over the deep basin. This was the region dominated by Atlantic origin water mixed with MW (the MW fraction increased by up to 15 %); the temperature was low, as was the fraction of RW (Figs. 4, 7).

Similar to the eastern Kara Sea, strong correlations were found between pCO_2 and temperature/salinity in the Laptev Sea, the recipient of the large Lena River inflow. The correlation was positive with temperature (R = 0.78) and negative with salinity (R = -0.59). The surface water salinity of the Laptev Sea was lower than that of the Kara Sea (Fig. 4) with the FW source dominated by riverine runoff (Fig. 7). Thus, higher pCO_2 values were found in the Laptev Sea than in the Kara Sea, including values as high as supersaturation.

Consequently, large areas of CO_2 out-gassing to the atmosphere were identified in the Laptev Sea, areas that might increase their strength as the climate warms. This is because when the permafrost thaws, more terrestrial OM will be exposed to microbial mineralization, producing CO_2 both within the drainage basins and in the river plume within the shelf sea. Photochemical transformation of terrestrial dissolved OM and direct photomineralization of OM also has an effect on increasing concentrations of CO_2 in surface waters (Bélanger et al., 2006; Fichot and Benner, 2014). The effect is strengthened by increased river discharge and by coastal erosion as a result of increasing water temperature and intensified wind and wave activity when the sea ice cover decreases (Serreze et al., 2007; Shakhova et al., 2014, 2015). Increasing ice-free water area leads to lower albedo and increased surface layer heating. Moreover, the supply of large quantities of optically active dissolved OM and suspended material (Dudarev et al., 2006; Sánchez-García et al., 2014; Vonk et al., 2014; Pugach and Pipko, 2013; Pugach et al., 2015; Charkin et al., 2015) also promotes the accumulation of solar radiation in the surface layer, which increases the heat content leading to further lengthening of the ice-free season (Granskog et al., 2007, 2015; Hill, 2008; Logvinova et al., 2016). Thus, water heating leads to additional increasing pCO_2 in the surface water. We also suggest that progression of subsea permafrost thawing and decrease in ice extent could result in a significant increase in carbon discharge from the sea floor (Nicolsky and Shakhova, 2010; Shakhova et al., 2014, 2015, 2017; Vonk et al., 2014) producing additional CO_2.

3.3.4 The East Siberian Sea

The surface water pCO_2 was in equilibrium with the atmosphere or slightly higher in the well-stratified waters of the East Siberian Sea. Supersaturation was observed not only in the shallow shelf sea, as previously described in literature (Anderson et al., 2009, 2011; Pipko et al., 2005, 2011b; Semiletov et al., 2007, 2012), but also in the adjacent deep-water area. The likely causes of the detected pCO_2 distribution are the anomalous dynamics of atmospheric processes, in particular the deep low-pressure area over land and high-pressure area over the ocean, as well as the sharp reduction in sea ice coverage. This led to RW being transported far to the north and northeast of the Eastern Arctic shelf and to intensive warming of the surface layer.

These waters carried a large amount of terrestrial OM to the deep sea, which would be further mineralized to CO_2 (Alling et al., 2010; Semiletov et al., 2016).

Surface water pCO_2 was somewhat higher at the oceanographic transect near the Lomonosov Ridge (the New Siberian Islands slope) than at the East Siberian Sea slope transect further to the east (Fig. 4); the pCO_2 of the East Siberian Sea slope transect was determined by different FW sources than was the pCO_2 of the Lomonosov Ridge. River runoff dominated as FW source to the western transect, while sea ice MW contributed a considerable volume to the eastern transect (Fig. 7). In addition, the use of a four-component mixing model reveals the possible presence of significant concentrations (up to 25 % or more) of Pacific-derived waters at the eastern transect (Abrahamsen et al., 2009; Bauch et al., 2011). The possibility of Pacific-derived waters penetrating to the eastern slope of the Lomonosov Ridge has been discussed before (Makhotin, 2010 and references therein). The climatological circulation during 1997-2006 that was reconstructed using the 4D variational approach shows the trajectories of several groups of Lagrangian particles (Shakhova et al., 2015); passive particles (or elements of the surface water mass) which originated in the eastern part of the East Siberian Sea between 160° and 170° E (the area impacted by the Pacific-derived waters) took less than two years to be transported to the Lomonosov Ridge area.

3.4 Dynamics of air-sea CO_2 fluxes in 2007

The air-sea CO_2 flux was computed with high spatial resolution along the cruise track from the Barents Sea to the East Siberian Sea (Fig. 9). Most of the studied areas of the ice-free waters served as a sink for atmospheric CO_2. Regions of intensive terrestrial impact in the Laptev Sea and the East Siberian Sea were the exception, and they acted as a weak source to the atmosphere (Fig. 9).

The Barents Sea is the strongest CO_2 sink in the Arctic region, yet estimates of the air-sea CO_2 flux in this area show large variability, depending on sub-region, season, and type of data used in the calculations (Lauvset et al., 2013). Using hourly averaged wind and cubic gas-transfer velocity parametrization (Wanninkhof and McGillis, 1999) we estimated the air-sea CO_2 flux in the least-explored sub-region of the sea. The highest rates of CO_2 uptake were found in the northeastern Barents Sea (160.9 mmol m^{-2} day^{-1}), where the high ΔpCO_2 (around -150 µatm) coincided with high daily wind speed (15 m sec^{-1}). It should be noted that air-sea CO_2 fluxes were low, on the order of 10 mmol m^{-2} day^{-1}, in the region between 35 and 45° E where the difference of pCO_2 values between sea and air was maximal (more than 150 µatm, Fig. 9), a result of the very low wind speed experienced here. A second region of the highest CO_2 invasion was detected in the northwestern Kara Sea, despite the fact that in this region ΔpCO_2 was almost two times lower (Fig. 9). Furthermore, the average CO_2 uptake rate was significantly greater in the Kara Sea than in the Barents Sea (50.7 versus 27.9 mmol m^{-2} day^{-1}, Table 1), despite the fact that average ΔpCO_2 was about half as much in the Kara Sea as it was in the Barents Sea (-46 µatm versus -94 µatm). The reason for this discrepancy is the wind speed, which averaged 9 m sec^{-1} in the Barents Sea and 14 m sec^{-1} in the Kara Sea (Fig. 9, Table 1). Hence, it is obvious that it is the wind speed that yields the large spatial flux patchiness, because this parameter is much more variable in

both time and space than is ΔpCO_2. In the eastern part of the Kara Sea, the CO_2 flux into the ocean was lower when the surface water pCO_2 was higher due to river discharge influence, which coincided with the weakening of the wind (Fig. 9).

In order to compare our estimates with those calculated by Lauvset et al. (2013), which carefully assessed the seasonal cycle of air-sea CO_2 fluxes in the Barents Sea, daily wind speed and quadratic parameterization of gas transfer velocity (Wanninkhof, 1992) were used for calculating CO_2 fluxes in the northern Barents Sea. The CO_2 flux into the seawater during fall 2007 reached an average of 126 g C m^{-2} year^{-1} and varied from 6 to 501 g C m^{-2} year^{-1}. Determined by low water temperature and high wind speed, the obtained values were close to the maximum average CO_2 uptake in the southern and central Barents Sea in highly productive spring months (April and May) (Lauvset et al., 2013). As the dataset by Lauvset et al. (2013) did not cover the north part of the sea comprehensively, the data obtained during our cruise adds information enabling a more accurate estimation of the absorption capacity of the whole Barents Sea in the fall season.

As noted before, there are both CO_2 sink and source regions in the Laptev and the East Siberian seas (Fig. 9). The southern Laptev Sea and the northwestern East Siberian Sea, where the terrestrial influence was significant and surface layer temperatures were the highest, served as a weak source of CO_2 to the atmosphere. However, even if there were regions of large ΔpCO_2 the fluxes were quite small (Fig. 9), a consequence of low winds; as a result the investigated area of the Laptev Sea as a whole was a weak sink for atmospheric CO_2 while that of the East Siberian Sea was a weak source of CO_2 to the atmosphere (Table 1).

3.5 The interannual variability of pCO_2 and air-sea CO_2 fluxes

3.5.1 The Barents and Kara seas

The surface layer of the Barents Sea was permanently undersaturated with respect to CO_2 and the ice-free waters were a sink of atmospheric CO_2, although the CO_2 flux was limited in the presence of sea ice cover (Figs. 3, 5, 9, Table 1). The lowest surface water pCO_2 was observed in 2009 under temperature conditions close to freezing; the mean value (170 µatm) was less than half that of the atmosphere. The mean pCO_2 value was higher in 2009 (189 µatm) with maximal magnitude in 2007 (280 µatm). Nevertheless, the CO_2 uptake was higher in 2006 and even higher in 2007 (Table 1). This is an effect of less sea ice cover during investigations in 2006 relative to 2009 (sea ice concentration in the study area was ~50 and 80 %, respectively) and lack of sea ice cover in 2007. The higher wind speed in 2007 was an additional driver which increased CO_2 uptake.

The Kara Sea was also a sink of CO_2 in 2006, 2007, and 2009, but to a variable degree, from close to zero in sea-ice-covered or RW-influenced areas to -170 mmol m^{-2} day^{-1} in western ice-free waters. The surface water pCO_2 at the two stations carried out in 2006 in the eastern part of the Kara Sea was slightly above 250 µatm (mean value = 259 µatm). Note that RW was not found in the eastern Kara Sea in 2006 (Fig. 7). That was determined by cyclonic atmospheric circulation (Fig. 2), which prevented spreading of the Ob and Yenisei river waters far to the east; sea ice MW was the main source of the FW in this region. The higher pCO_2 in 2007, increased from 284 to 372 µatm, was associated with higher sea surface temperature and the presence of RW in the eastern part of the sea (Figs. 4, 7). Minimal surface pCO_2 (mean value 206 µatm) was revealed in 2009

(Fig. 5). Nevertheless, the average CO_2 uptake rate was the highest in 2007 (Table 1). Once again this is a result of the fact that the main part of the study area in 2009 was in ice-covered waters while most of the 2007 cruise was in open water (Fig. 1); the wind was also stronger in 2007.

This finding stresses the importance of declining sea ice coverage and strengthening wind for the ocean's ability to take up atmospheric CO_2 in northern parts of the Barents and Kara seas mainly remote from direct terrestrial discharge.

3.5.2 The Laptev and East Siberian seas

The most extensive study over the three years was conducted in the Laptev Sea and in the northwestern East Siberian Sea, the region where negative September ice concentration anomalies were most pronounced for the whole Arctic Ocean (ftp://sidads.colorado.edu). Surface waters of the outer shelf and slope in 2006 and 2009 were undersaturated in CO_2 relative to the atmosphere; 2007 was an exception (Table 1).

For comparative evaluation, we selected a transect north of the New Siberian Islands over the Lomonosov Ridge (Figs. 1, 10). Note that pCO_2 data of the selected transect, reported in Fig 10, were calculated for discrete samples (from A_T, pH_T20, and inorganic nutrients data) by means of the CO2SYS program of Lewis and Wallace (1998).

The salinity distribution along the transect during the three cruises shows a similar general pattern, but with some significant variations especially in the top 30-50 m (Fig. 10). Of the three years, 2007 had the lowest surface salinity and the most pronounced halocline (Fig. 10). However, the largest interannual differences were in the seawater temperature distribution. In late summer 2007 the surface layer was the warmest and was underlain by a sharp thermocline coinciding in depth with the halocline to form a strong pycnocline that restricted vertical exchange. A characteristic feature of the vertical distribution of pCO_2 along the transect in late summer 2007 was a pronounced subsurface maximum of pCO_2 (Fig. 10) and higher pCO_2 values in the surface waters. The subsurface maximum was found exactly at the slope, and coincided with a layer of brine-enriched southeastern Laptev Sea bottom waters (Bauch et al., 2011). During years with prevalent offshore wind, such brine-enriched waters are exported to the Arctic Ocean halocline at about 50 m water depth (Bauch et al., 2009, 2011).

Westerly winds during the ice-free period in summer 2007 advected the Lena River plume to the northeast. Thus, the low salinity was mainly related to the effective transfer of RW into the deep ocean due to the wind field and ice-free conditions, but salinity was also somewhat impacted by higher river discharge in 2007 (an average of 752, 822, and 738 km^3 for the Lena and Kolyma rivers in 2006, 2007, and 2009, respectively). The calculated RW content in the surface layer reached over 30 % in 2007, but did not exceed 20 % in 2006 or 10 % in 2009 (Fig. 11). Distribution of normalized A_T also confirmed the presence of a large amount of RW in 2007 (Fig. 11). The content of brine (indicating negative sea ice MW) in the surface water was also significantly higher during summer 2007 compared to the fall of 2006 and 2009 (Figs. 7, 11). This part of the Laptev Sea is known as a large sea ice production region and thus the brine signature builds up during the winter season. One consequence is that little sea ice MW was observed, up to a maximum of only 5 %, even though sea ice melt decreases the brine signal in the summer. The maximum MW fraction was in the low salinity range of the surface water at the southern end of the section in 2006 (Figs. 7, 10, 11).

The substantial impact by river discharge in 2007 was characterized by high pCO_2, resulting in weak oversaturation in the south of the transect. Thus, ΔpCO_2 conditions (Table 1) favoring CO_2 out-gassing into the atmosphere were observed even on the northern edge of the outer shelf (Fig. 10). This situation is not typical for the deep waters of the Laptev Sea because the outer shelf normally acts as a sink for atmospheric CO_2, unlike the middle and inner shelves (Semiletov et al., 2007; Anderson et al., 2009; Pipko et al., 2016).

The pCO_2 in the lowest-salinity surface water was around 270 and 300 µatm in 2006 and 2009, respectively, although the runoff source ranged between 10 and 20 %. The higher CO_2 content of river runoff in 2007 not only contributed to high pCO_2 but also enhanced surface water temperature due to its high concentration of CDOM, which adsorbs solar radiation (Pugach et al., 2015; Semiletov et al., 2013). Except for the lower runoff content compared to 2007 the main contribution to the pCO_2 interannual variability was seawater temperature that was about 4 °C higher in 2007 (Fig. 10).

In summary, the strength and direction of air-sea CO_2 fluxes on the outer shelf and continental slope of the Laptev and the East Siberian seas varied significantly among years (Figs. 4, 5, 9, Table 1). The area was a sink of atmospheric CO_2 in 2006 and 2009, and the surface water of the East Siberian Sea was a weak source in 2007 (Table 1). That change from sink to source was related to the distribution of the RW plume on the shelf, the transport of terrestrial OM (and its oxidation to CO_2) by this plume, and the plume's impact on water temperature, as well as sea ice extent and wind speed (Fig. 1, Table 1). It should be noted that pCO_2 was higher in the deep regions of the Laptev and East Siberian seas than in the deep regions of the Kara Sea, even if the discharge is higher in the Kara Sea than in the ESAS. This is likely a combination of the dominating flow of the river plume and the source pCO_2 in the water that mixes with the runoff; the water in the Kara Sea comes from the Barents Sea with its low pCO_2, while the Laptev Sea is dominated by inflow from the Kara Sea.

4 Conclusions

This three-year study of the outer shelf and the continental slope waters of the Eurasian Arctic seas has revealed a general trend in the surface pCO_2 distribution, which manifested as an increase in pCO_2 values eastward, from the surface waters of the highly productive Barents Sea to the poorly productive eastern Laptev Sea and western East Siberian Sea, which are strongly influenced by terrestrial runoff and coastal/subsea permafrost erosion. It has been shown that the influence of terrestrial discharge on the carbonate system of East Siberian Arctic seas surface waters is not limited to the shallow shelf. Furthermore, during certain meteorological conditions, the surface waters of the outer shelf, as well as those of the continental slope of the East Siberian Arctic seas, can become supersaturated with respect to atmospheric CO_2.

Contemporary climate change affects air temperature in the Arctic region leading to sea-ice reduction and permafrost thawing, both on-land and off-shore. Increasing air temperatures cause increased water temperature and strengthened wind activity, which intensifies water mass dynamics and air-sea exchange. It was shown that these changes in the Arctic climatology can affect the capacity of this region to serve as a source or a sink for atmospheric CO_2 in two opposite ways. On the one hand, larger areas of open water due to sea ice reduction and longer ice-free periods can cause the outer shelf and slope of the West

475 Siberian Eurasian Arctic seas (Barents and Kara seas) to develop a growing capability to absorb atmospheric CO_2; on the other hand, growing river discharge and degradation of permafrost, associated with thermal erosion of coasts and river banks, can increase the effectiveness of the East Siberian Arctic seas to act as a CO_2 source due to increased terrestrial export of labile eroded carbon, a significant portion of which oxidizes to CO_2. This was the situation in the deep regions of the Laptev and East Siberian seas in 2007, when sea ice decline was especially pronounced, resulting in an increase of the area where seawater

480 pCO_2 was in equilibrium or slightly supersaturated with respect to atmosphere and a reduction of CO_2 absorption in the East Siberian Arctic seas.

This study has shown that contemporary climate change impacts the carbon cycle of the Eurasian Arctic Ocean and influences air-sea CO_2 flux. It also highlights the importance of considering small-scale variations in meteorological and hydrological parameters, varying both in time and in space, for estimating the air-sea exchange of CO_2. During these times of rapid

485 environmental changes, results of this study stress the need for comprehensive multi-year investigations of dynamic deep-sea regions in order to estimate current and predict future capacity of the Arctic basin as a sink for atmospheric CO_2 based on high-resolution spatial coverage of the Arctic Ocean.

Acknowledgements

490 This work was supported by the Russian Government (grant 14.Z50.31.0012); the Far Eastern Branch of the Russian Academy of Sciences (FEBRAS); the International Arctic Research Center (IARC) of the University of Alaska Fairbanks through NOAA Cooperative Agreement NA17RJ1224; the U.S. National Science Foundation (Nos. OPP-0327664, OPP-0230455, ARC-1023281, ARC-0909546); and the NOAA OAR Climate Program Office (NA08OAR4600758). I.P. and S.P. acknowledge the Russian Foundation for Basic Research (No. 14-05-00433a). L.G.A. and Ö.G. thank the Swedish Research Council and the Knut and Alice Wallenberg Foundation, as well as the European Research Council (ERC-AdG CC-TOP project #695331 to

495 Ö.G.). N.S., O.D., I.P., and A.Ch. thank the Russian Science Foundation (grant No. 15-17- 20032). I.P., S.P., and I.S. would like to thank Dr. P.Ya. Tishchenko for collaboration and useful comments. We also thank two anonymous reviewers for their constructive comments, which improved the manuscript. We thank Candace O'Connor for English editing.

Data availability. Data are available upon request to the corresponding author.

500

Competing interests. The authors declare that they have no conflict of interest.

505

References

Abrahamsen, E. P., Meredith, M. P., Falkner, K. K., Torres-Valdes, S., Leng, M. J., Alkire, M. B., Bacon, S., Laxon, S. W., Polyakov, I., and Ivanov, V.: Tracer-derived freshwater budget of the Siberian Continental Shelf following the extreme Arctic summer of 2007, Geophys. Res. Lett., 36, L07602, doi:10.1029/2009GL037341, 2009.

Alling, V., Sánchez-García, L., Porcelli, D., Pugach, S., Vonk, J., van Dongen, B., Mörth, C. M., Anderson, L. G., Sokolov, A., Andersson, P., Humborg, C., Semiletov, I., and Gustafsson, Ö.: Nonconservative behavior of dissolved organic carbon across the Laptev and East Siberian seas, Global Biogeochem. Cy., 24, GB4033, doi:10.1029/2010GB003834, 2010.

Anderson, L. G., Olsson, K., and Chierici, M.: A carbon budget for the Arctic Ocean, Global Biogeochem. Cy., 12, 455–465, 1998.

Anderson, L. G., Jutterström, S., Hjalmarsson, S., Wåhlström, I., and Semiletov, I. P.: Out-gassing of CO_2 from Siberian shelf seas by terrestrial organic matter decomposition, Geophys. Res. Lett., 36, L20601, doi: http://dx.doi.org/10.1029/2009GL040046, 2009.

Anderson, L. G., Björk, G., Jutterström, S., Pipko, I., Shakhova, N., Semiletov, I., and Wåhlström, I.: East Siberian Sea, an Arctic region of very high biogeochemical activity, Biogeosciences, 8, 1745-1754, doi:10.5194/bg-8-1745-2011, 2011.

Anderson, L. G., Ek, J., Ericson, Y., Humborg, C., Semiletov, I., Sundbom, M., and Ulfsbo, A.: Export of calcium carbonate corrosive waters from the East Siberian Sea, Biogeosciences, 14, 1811-1823, doi:10.5194/bg-14-1811-2017, 2017.

Årthun, M., Bellerby, R. G. J., Omar, A. M., and Schrum, C.: Spatiotemporal variability of air–sea CO_2 fluxes in the Barents Sea, as determined from empirical relationships and modeled hydrography, J. Marine Syst., 98-99, 40–50, 2012.

Bates, N.R.: Air–sea CO_2 fluxes and the continental shelf pump of carbon in the Chukchi Sea adjacent to the Arctic Ocean, J. Geophys. Res., 111, C10013, 10.1029/2005JC003083, 2006.

Bates, N. R. and Mathis, J. T.: The Arctic Ocean marine carbon cycle: evaluation of air-sea CO_2 exchanges, ocean acidification impacts and potential feedbacks, Biogeosciences, 6, 2433–2459, doi: 10.5194/bg-6-2433-2009, 2009.

Bauch, D., Dmitrenko, I. A., Wegner, C., Hölemann, J., Kirillov, S. A., Timokhov, L. A., and Kassens H.: Exchange of Laptev Sea and Arctic Ocean halocline waters in response to atmospheric forcing, J. Geophys. Res., 114, C05008, 2009.

Bauch, D., Groger, M., Dmitrenko, I., Holemann, J., Kirillov, S., Mackensen, A., Taldenkova, E., and Andersen, N.: Atmospheric controlled freshwater release at the Laptev Sea continental margin, Polar Res., 30, 5858, doi: 10.3402/polar.v30i0.5858, 2011.

Bélanger, S., Xie, H., Krotkov, N., Larouche, P., Vincent, W. F., and Babin, M.: Photomineralization of terrigenous dissolved organic matter in Arctic coastal waters from 1979 to 2003: Interannual variability and implications of climate change, Global Biogeochem. Cycles, 20, GB4005, doi:10.1029/2006GB002708, 2006.

Bhatt, U. S., Walker, D. A., Raynolds, M. K., Comiso, J. C., Epstein, H. E., Jia, G., Gens, R., Pinzon, J. E., Tucker, C. J., Tweedie, C. E., and Webber, P.J.: Circumpolar Arctic tundra vegetation change is linked to sea-ice decline, Earth Interact., 14, doi: http://dx.doi.org/10.1175/2010EI315.1, 2010.

540 Bischoff, J., Sparkes, R. B., Doğrul, S. A., Spencer, R. G. M., Gustafsson, Ö., and Semiletov, I. P.: Source, transport and fate of soil organic matter inferred from microbial biomarker lipids on the East Siberian Arctic Shelf, Biogeosciences, 13, 4899–4914, 2016.

Bröder, L., Tesi, T., Salvadó, J. A., Semiletov, I. P., Dudarev, O. V., and Gustafsson, Ö.: Fate of terrigenous organic matter across the Laptev Sea from the mouth of the Lena River to the deep sea of the Arctic interior, Biogeosciences, 13, 5003-5019, 2016.

545 Bruevich, S. V.: Instruction for Chemical Investigation of Seawater, Glavsevmorput, Moscow, 83 pp., 1944 (in Russian).

Carmack, E., Barber, D., Christensen, J., Macdonald, R., Rudels, B., and Sakshaug, E.: Climate variability and physical forcing of the food webs and the carbon budget on panarctic shelves, Prog. Oceanogr., 71, 145–181, 2006.

Charkin, A. N., Dudarev, O. V., Shakhova, N. E., Semiletov, I. P., Pipko, I. I., Pugach, S. P., and Sergienko, V.I.: Peculiarities of the formation of suspended particulate matter fields in the eastern Arctic seas, Dokl. Earth Sci., 462, 626–630, 2015.

550 DeGrandpre, M. D., Hammar, T. R., Smith, S. P., and Sayles, F. L.: In-situ measurements of seawater pCO_2, Limnol. Oceanogr., 40, 969–975, 1995.

Dickson, A. G.: Standard potential of the reaction: $AgCl(s) + 1/2 H2(g) = Ag(s) + HCl(aq)$, and the standard acidity constant of the ion $HSO4^-$ in synthetic sea water from 273.15 to 318.15 K, Journal of Chemical Thermodynamics, 22, 113-127, 1990a.

Dickson, A. G.: Thermodynamics of the dissolution of boric acid in synthetic seawater from 273.15°K to 318.15°K, Deep Sea Res., Part A, 37(5), 755‑766, 1990b.

Dickson, A. G. and Millero, F. J.: A comparison of the equilibrium constants for the dissociation of carbonic acid in seawater media, Deep-Sea Res., 34, 1733-1743, 1987.

Dickson, A. G., Sabine, C. L., and Christian, J. R.: Guide to best practices for ocean CO_2 measurements, PICES Special Publication 3, IOCCP Report no. 8, 2007.

560 Dittmar, T. and Kattner, G.: The biogeochemistry of the river and shelf ecosystem of the Arctic Ocean: A review, Mar. Chem., 83, 103–120, 2003.

DOE: Handbook of Methods for the Analysis of the Various Parameters of the Carbon Dioxide System in Sea Water, Version 2, edited by: Dickson, A. G. and Goyet, C., 1994.

Dudarev, O. V., Semiletov, I. P., and Charkin, A. N.: Particulate material composition in the Lena River-Laptev Sea system: scales of heterogeneities, Dokl. Earth Sci., 411A, 1445–1451, 2006.

Ekwurzel, B., Schlosser, P., Mortlock, R., and Fairbanks, R.: River runoff, sea-ice meltwater, and Pacific water distribution and mean residence times in the Arctic Ocean, J. Geophys. Res. - Oceans, 106, 9075-9092, 2001.

Fichot, C. G., and Benner, R.: The fate of terrigenous dissolved organic carbon in a river-influenced ocean margin, Global Biogeochem. Cycles, 28, doi:10.1002/2013GB004670, 2014.

570   Findlay, H. S., Gibson, G., Kedra, M., Morata, N., Orchowska, M., Pavlov, A. K., Reigstad, M., Silyakova, A., Tremblay, J.-E., Walczowski, W., Weydmann, A., and Logvinova, C.: Responses in Arctic marine carbon cycle processes: conceptual scenarios and implications for ecosystem function, Polar Res., 34, 24252, http://dx.doi.org/10.3402/polar.v34.24252, 2015.

Fransson, A., Chierici, M., Anderson, L. G., Bussmann, I., Kattner, G., Jones, E. P., and Swift, J. H.: The importance of shelf processes for the modification of chemical constituents in the waters of the Eurasian Arctic Ocean: implication for carbon

575   fluxes, Cont. Shelf Res., 21, 225–242, 2001.

Fransson, A., Chierici, M., and Nojiri, Y.: New insights into the spatial variability of the surface water carbon dioxide in varying sea-ice conditions in the Arctic Ocean, Cont. Shelf Res., 29, 1317–1328, doi:10.1016/j.csr.2009.03.008, 2009.

Granskog, M. A., Macdonald, R. W., Mundy, C. J., and Barber, D. G.: Distribution, characteristics and potential impacts of chromophoric dissolved organic matter (CDOM) in Hudson Strait and Hudson Bay, Canada, Cont. Shelf Res., 27, 2032–2050,

580   2007.

Granskog, M. A., Pavlov, A. K., Sagan, S., Kowalczuk, P., Raczkowska, A., and Stedmon, C. A.: Effect of sea-ice melt on inherent optical properties and vertical distribution of solar radiant heating in Arctic surface waters, J. Geophys. Res. Oceans, 120, doi:10.1002/2015JC011087, 2015.

Gustafsson, Ö., van Dongen, B. E., Vonk, J. E., Dudarev, O. V., and Semiletov, I. P.: Widespread release of old carbon across

585   the Siberian Arctic echoed by its large rivers, Biogeosciences, 8, 1737–1743, doi:10.5194/bg-8-1737-2011, 2011.

Harms, I. H. and Karcher, M. J.: Modeling the seasonal variability of hydrography and circulation in the Kara Sea, J. Geophys. Res., 104, 13431-13448, 1999.

Hill, V. J.: Impacts of chromophoric dissolved organic material on surface ocean heating in the Chukchi Sea, J. Geophys. Res., 113, C07024. http://dx.doi. org/10.1029/2007JC004119, 2008.

590   Holmes, R. M., McClelland, J.W., Peterson, B. J., Tank, S. E., Bulygina, E., Eglinton, T. I., Gordeev, V. V., Gurtovaya, T. Y., Raymond, P. A., Repeta, D. J., Staples, R., Striegl, R. G., Zhulidov, A. V., and Zimov, S. A.: Seasonal and Annual Fluxes of Nutrients and Organic Matter from Large Rivers to the Arctic Ocean and Surrounding Seas, Estuaries and Coasts 35, 369–382, 2012.

Hopkins, T. S.: The GIN Sea - a synthesis of its physical oceanography and literature review 1972–1985, Earth-Sci. Rev., 30,

595   175–318, 1991.

Jakobsson, M.: Hypsometry and volume of the Arctic Ocean and its constituent seas, Geochem. Geophys. Geosyst., 3, 1028, doi:10.1029/2001GC000302, 2002.

Jeffries, M. O., Overland, J. E., and Perovich, D. K. The Arctic shifts to a new normal, Phys. Today, 66 (10), 35, doi: 10.1063/PT.3.2147, 2013.

600   Kaltin, S., Anderson, L. G., Olsson, K., Fransson, A., and Chierici, M.: Uptake of atmospheric carbon dioxide in the Barents Sea, J. Mar. Syst., 38, 31–45, 2002.

Karlsson, E., Gelting, J., Tesi, T., van Dongen, B., Semiletov, I., Charkin, A., Dudarev, O., and Gustafsson, Ö.: Different sources and degradation status of dissolved, particulate and sedimentary organic matter along the Eurasian Arctic coastal margin, Global Biogeoch. Cy., 30, 898-916, 2016.

605   Kattsov, V., Ryabinin, V., Overland, J., Serreze, M., Visbeck, M., Walsh, J., Meier, W., and Zhang, X.: Arctic sea-ice change: A grand challenge of climate science, J. Glaciol., 56, 1115–1121, doi:10.3189/ 002214311796406176, 2010.

Lauvset, S. K., Chierici, M., Counillon, F., Omar, A., Nondal, G., Johannessen, T., and Olsen, A.: Annual and seasonal fCO_2 and air–sea CO_2 fluxes in the Barents Sea, J. Mar. Syst., 113–114, 62–74, 2013.

Lewis, E. and Wallace, D. W. R.: Program developed for CO_2 system calculations. ORNL/CDIAC-105. Carbon Dioxide

610   Information Analysis Center. Oak Ridge National Laboratory, US Department of Energy, Oak Ridge, Tennessee, 1998.

Loeng, H.: Features of the physical oceanographic conditions of the Barents Sea. In: Sakshaug, E., Hopkins, C. C. E., and Øritsland, N. A. (Eds.), Proceedings of the Pro Mare symposium on Polar Marine Ecology, 5–18, 1991.

Logvinova, C. L., Frey, K.E., and Cooper, L.W.: The potential role of sea ice melt in the distribution of chromophoric dissolved organic matter in the Chukchi and Beaufort Seas, Deep-Sea Research II, 130, 28–42, 2016.

615   Macdonald, R. W., Anderson, L. G., Christensen, J. P., Miller, L. A., Semiletov, I. P., and Stein, R.: The Arctic Ocean: budgets and fluxes, in: Carbon and Nutrient Fluxes in Continental Margins: A Global Synthesis, Edited by Liu, K.-K., Atkinson, L., Quinones, R., and Talaue-McManus, L., Springer-Verlag, 291-303, 2008.

Makhotin, M. S.: Distribution of pacific summer waters in the Arctic Ocean, Problemi Arktiki I Antarktiki, 86, 3, 89-96, 2010 (in Russian).

620   Makkaveev, P. N., Stunzhas, P.A., and Khlebopashev, P. V.: The distinguishing of the Ob and Yenisei waters in the desalinated lenses of the Kara Sea in 1993 and 2007, Oceanology, 50, 698-705, doi: 10.1134/S0001437010050073, 2010.

Makkaveev, P. N., Melnikova, Z. G., Polukhin, A. A., Stepanova, S. V., Khlebopashev, P. V., and Chultsova, A. L.: Hydrochemical characteristics of the waters in the western part of the Kara Sea, Oceanology, 55, 485-496, doi: 10.1134/S0001437015040116, 2015.

625   Mann, P. J., Davydova, A., Zimov, N., Spencer, R. G. M., Davydov, S., Bulygina, E., Zimov, S., and Holmes, R. M.: Controls on the composition and lability of dissolved organic matter in Siberia's Kolyma River basin, J. Geophys. Res., 117, G01028, doi:10.1029/2011JG001798, 2012.

Mann, P. J., Eglinton, T. I., McIntyre, C. P., Zimov, N., Davydova, A., Vonk, J. E., Holmes, R. M., and Spencer, R. G. M.: Utilization of ancient permafrost carbon in headwaters of Arctic fluvial networks, Nature Communications, 6, 7856, doi:

630   10.1038/ncomms8856, 2015.

Mehrbach, C., Culberson, C. H., Hawley, J. E., and Pytkowicz, R. M.: Measurements of the apparent dissociation constants of carbonic acid in seawater at atmospheric pressure, Limnol. Oceanogr., 18, 897-907, 1973.

Nakaoka, S., Aiki, S., Nakazawa, T., Hashida, G., Morimoto, S., Yamanouchi, T., and Yoshikawa-Inoue, H.: Temporal and spatial variations of oceanic pCO_2 and air–sea CO_2 flux in the Greenland Sea and the Barents Sea, Tellus, 58, 148–161, 2006.

635   Nedashkovsky, A. P. and Shvetsova, M. G.: Total inorganic carbon in sea-ice, Oceanology, 50, 861-868, 2010.

Nicolsky, D. and Shakhova, N.E.: Modeling sub-sea permafrost in the East Siberian Arctic Shelf: the Dmitry Laptev Strait, Environmental Research Letters, 5, 015006, 2010.

Olsson, K., and Anderson, L. G.: Input and biogeochemical transformation of dissolved carbon in the Siberian shelf seas, Cont. Shelf Res., 17, 819-833, 1997.

640   Omar, A. M., Johannessen, T., Olsen, A., Kaltin, S., and Rey, F.: Seasonal and interannual variability of the air–sea CO_2 flux in the Atlantic sector of the Barents Sea, Mar. Chem., 104, 203–213, 2007.

Overland, J. E., Wang, J., Pickart, R. S., and Wang, M.: Recent and Future Changes in the Meteorology of the Pacific Arctic, Grebmeier, J. M. and Maslowski, W. (eds.), The Pacific Arctic Region: Ecosystem Status and Trends in a Rapidly Changing Environment, doi: 10.1007/978-94-017-8863-22, Springer Science+Business Media Dordrecht, 17-30, 2014.

645   Pavlova, G. Yu., Tishchenko, P. Ya., Volkova, T. I., Dickson, A., and Wallmann, K.: Intercalibration of Bruevich's method to determine the total alkalinity in seawater, Oceanology, 48, 3, 438–443, 2008.

Pipko, I. I., Semiletov, I. P., Tishchenko, P. Ya., Pugach, S. P., and Christensen, J. P.: Carbonate chemistry dynamics in Bering Strait and the Chukchi Sea, Progress in Oceanography, 55, 1-2, 77-94, 2002.

Pipko, I. I., Semiletov, I. P., and Pugach S. P.: The carbonate system of the East Siberian Sea waters, Dokl. Earth Sci., 402,
650   624–627, 2005.

Pipko, I. I., Pugach, S. P., Semiletov, I. P., and Salyuk, A. N.: Carbonate characteristics of waters of the Arctic Ocean continental slope, Dokl. Earth Sci., 438, 858-863, 2011a.

Pipko, I. I., Semiletov, I. P., Pugach, S. P., Wåhlström, I., and Anderson, L. G.: Interannual variability of air-sea CO_2 fluxes and carbon system in the East Siberian Sea, Biogeosciences, 8, 1987-2007, doi:10.5194/bg-8-1987-2011, 2011b.

655   Pipko, I. I., Pugach, S. P., and Semiletov, I. P.: Characteristic features of the dynamics of carbonate parameters in the Eastern part of the Laptev Sea, Oceanology, 55, 68–81, 2015.

Pipko, I. I., Pugach, S. P., and Semiletov, I. P.: Assessment of the CO_2 fluxes between the ocean and the atmosphere in the eastern part of the Laptev Sea in the ice-free period, Dokl. Earth Sci., 467, 398–401, 2016.

Pitzer, K. S.: Ionic interaction approach: theory and data correlation. In: Pitzer, K.S. (Ed.), Activity Coefficients in Electrolyte
660   Solutions second ed. CRC Press, London, pp. 75–153, 1991.

Pugach, S. P. and Pipko, I. I.: Dynamic of colored dissolved organic matter on the East-Siberian Sea shelf, Dokl. Earth Sci., 448, 1, 153-156, 2013.

Pugach, S. P., Pipko, I. I., Semiletov, I. P., and Sergienko, V. I.: Optical characteristics of the colored dissolved organic matter on the East Siberian Shelf, Dokl. Earth Sci., 465, 1293–1296, 2015.

665   Pugach, S. P., Pipko, I. I., Shakhova, N. E., Shirshin, E. A., Perminova, I. V., Gustafsson, Ö., Bondur, V. G., and Semiletov, I. P.: DOM and its optical characteristics in the Laptev and East Siberian seas: Spatial distribution and inter-annual variability (2003–2011), Ocean Sci. Discuss., https://doi.org/10.5194/os-2017-20, 2017.

Raymond, P. A., McClelland, J. W., Holmes, R. M., Zhulidov, A. V., Mull, K., Peterson, B. J., Striegl, R. G., Aiken, G. R., and Gurtovaya, T. Y.: Flux and age of dissolved organic carbon exported to the Arctic Ocean: A carbon isotopic study of the five largest arctic rivers, Global Biogeochem. Cy., 21, GB4011, doi:10.1029/2007GB002934, 2007.

Rysgaard, S., Glud, R. N., Lennert, K., Cooper, M., Halden, N., Leakey, R. J. G., Hawthorne, F. C., and Barber, D.: Ikaite crystals in melting sea-ice – implications for pCO_2 and pH levels in Arctic surface waters, The Cryosphere, 6, 1–8, 2012.

Sánchez-García, L., Vonk, J. E., Charkin, A. N., Kosmach, D., Dudarev, O. V., Semiletov, I. P., and Gustafsson, Ö.: Characterisation of three regimes of collapsing Arctic ice complex deposits on the SE Laptev Sea coast using biomarkers and dual carbon isotopes, Permafrost Periglac., 25, 172–183, 2014.

Schauer, U., Loeng, H., Rudels, B., Ozhigin, V. K., and Dieck, W.: Atlantic water flow through the Barents and Kara Seas, Deep-Sea Res. I, 49, 2281–2298, 2002.

Schirrmeister, L., Grosse, G., Wetterich, S., Overduin, P. P., Strauss, J., Schuur, E. A. G., and Hubberten, H.-W.: Fossil organic matter characteristics in permafrost deposits of the northeast Siberian Arctic, J. Geophys. Res., 116, G00M02, doi:10.1029/2011JG001647, 2011.

Schlitzer, R.: Ocean Data View, http://odv.awi.de, 2011.

Semiletov, I. P.: Destruction of the coastal permafrost as an important factor in biogeochemistry of the Arctic shelf waters, Dokl. Earth Sci., 368, 679–682, 1999.

Semiletov, I. P., Savelieva, N. I., Weller, G. E., Pipko, I. I., Pugach, S. P., Gukov, A. Y., and Vasilevskaya, L. N.: The dispersion of Siberian river flows into coastal waters: Meteorological, hydrological and hydrochemical Aspects, in: The Freshwater Budget of the Arctic Ocean, edited by: Lewis, E. L., Jones, E. P., Lemke, P., Prowse, T. D., and Wadhams, P., 323–366, Springer Netherlands, Dordrecht, doi:10.1007/978-94-011-4132-1_15, 2000.

Semiletov, I. P., Pipko, I. I., Repina, I., and Shakhova, N. E.: Carbonate chemistry dynamics and carbon dioxide fluxes across the atmosphere-ice-water interfaces in the Arctic Ocean: Pacific sector of the Arctic, J. Marine Syst., 66, 204–226, 2007.

Semiletov, I. P., Shakhova, N. E., Sergienko, V. I., Pipko, I. I., and Dudarev, O. V.: On carbon transport and fate in the East Siberian Arctic land-shelf-atmosphere system, Environ. Res. Lett., 7, 015201, doi: 10.1088/1748-9326/7/1/015201, 2012.

Semiletov, I. P., Shakhova, N. E., Pipko, I. I., Pugach, S. P., Charkin, A. N., Dudarev, O. V., Kosmach, D.A., and Nishino, S.: Space-time dynamics of carbon and environmental parameters related to carbon dioxide emissions in the Buor-Khaya Bay and adjacent part of the Laptev Sea, Biogeosciences, 10, 5977-5996, doi: 10.5194/bg-10-5977-2013, 2013.

Semiletov, I., Pipko, I., Gustafsson, Ö., Anderson, L. G., Sergienko, V., Pugach, S., Dudarev, O., Charkin, A., Gukov, A., Bröder, L., Andersson, A., Spivak, E., and Shakhova, N.: Acidification of East Siberian Arctic Shelf waters through addition of freshwater and terrestrial carbon, Nature Geosci., 9, 361-365, doi: 10.1038/ngeo2695, 2016.

Serreze, M. C. and Barry, R. G.: Processes and impacts of Arctic amplification: A research synthesis, Global Planet. Change, 77, 85–96, 2011.

Serreze, M. C., Holland, M. M., and Stroeve, J.: Perspectives on the Arctic's shrinking sea-ice cover, Science, 315, 5818, 1533-1536, doi: 10.1126/science.1139426, 2007.

Shakhova, N., Sergienko, V., and Semiletov, I.: The contribution of the East Siberian shelf to the modern methane cycle, Herald of the Russian Academy of Sciences, 79, 1, 237 – 246, 2009.

Shakhova, N., Semiletov, I., Leifer, I., Sergienko, V., Salyuk, A., Kosmach, D., Chernikh, D., Stubbs, Ch., Nicolsky, D., Tumskoy, V., and Gustafsson, Ö.: Ebullition and storm-induced methane release from the East Siberian Arctic Shelf, Nature Geosci., 7, 64-70, 2014.

Shakhova, N., Semiletov, I., Sergienko, V., Lobkovsky, L., Yusupov, V., Salyuk, A., Salomatin, A., Chernykh, D., Kosmach, D., Panteleev, G., Nicolsky, D., Samarkin, V., Joye, S., Charkin, A., Dudarev, O., Meluzov, A., and Gustafsson, Ö.: The East Siberian Arctic Shelf: towards further assessment of permafrost-related methane fluxes and role of sea-ice, Phil. Trans. R. Soc. A, 373, 20140451, 2015.

Shakhova, N., Semiletov, I., Gustafsson, O., Sergienko, V., Lobkovsky, L., Dudarev, O., Tumskoy, T., Grigoriev, M., Mazurov, A., Salyuk, A., Ananiev, R., Koshurnikov, A., Kosmach, D., Charkin, A., Dmitrevsky, N., Karnaukh, V., Gunar, A., Meluzov, A., and Chernykh, D.: Current rates and mechanisms of subsea permafrost degradation in the East Siberian Arctic Shelf, Nature Communications, 8, 15872, doi: 10.1038/ncomms15872, 2017.

Stroeve, J. C., Serreze, M. C., Holland, M. M., Kay, J. E., Malanik, J., and Barrett, A. P.: The Arctic's rapidly shrinking sea-ice cover: a research synthesis, Climatic Change, 110, 1005–1027, 2012.

Stroeve, J. C., Markus, T., Boisvert, L., Miller, J., and Barrett, A.: Changes in Arctic melt season and implications for sea-ice loss, Geophys. Res. Lett., 41, 1216–1225, doi:10.1002/2013GL058951, 2014.

Takahashi, T., Olafsson, J., Goddard, J. G., Chipman, D. W., and Sutherland, S. C.: Seasonal variation of CO_2 and nutrients in the high latitude surface oceans: a comparative study, Global Biogeochem. Cy., 7, 843–878, 1993.

Tank, S. E., Raymond, P. A., Striegl, R. G., McClelland, J. W., Holmes, R. M., Fiske, G. J., and Peterson, B. J.: A land-to-ocean perspective on the magnitude, source and implication of DIC flux from major Arctic rivers to the Arctic Ocean, Global Biogeochem. Cy., 26, GB4018, doi:10.1029/2011GB004192, 2012.

Tesi, T., Semiletov, I., Hugelius, G., Dudarev, O., Kuhry, P., and Gustafsson, Ö.: Composition and fate of terrigenous organic matter along the Arctic land–ocean continuum in East Siberia: Insights from biomarkers and carbon isotopes, Geochim. Cosmochim. Acta, 133, 235–256, 2014.

Tesi, T., Semiletov, I., Dudarev, O., Andersson, A., and Gustafsson, Ö.: Matrix association effects on hydrodynamic sorting and degradation of terrestrial organic matter during cross-shelf transport in the Laptev and East Siberian shelf seas, J. Geophys.Res. - Biogeosci., 121, doi:10.1002/2015JG003067, 2016.

Tishchenko, P. Ya.: Non-ideal properties of the TRIS–TRIS - HCl–NaCl–H2O buffer system in the 0-40 °C temperature interval. Application of the Pitzer equations, Izv. Akad. Nayk. Ser. Khim., 49, 670–675, 2000 (in Russian).

Tishchenko, P. Ya., Wong, C. S., Pavlova, G. Yu., Johnson, W. K., Kang, D.-J., and Kim, K.-R.: The measurement of pH values in seawater using a cell without a liquid junction, Oceanology, 41, 813–822, 2001.

Tishchenko, P. Ya., Kang, D.-J., Chichkin, R. V., Lazaryuk, A. Yu., Wong, C. Sh., and Johnson, W. K.: Application of potentiometric method using a cell without liquid junction to underway pH measurements in surface seawater, Deep-Sea Res. I, 58, 778–786, 2011.

Vonk, J. E., Semiletov, I. P., Dudarev, O. V., Eglinton, T. I., Andersson, A., Shakhova, N., Charkin, A., Heim, B., and Gustafsson, Ö.: Preferential burial of permafrost-derived organic carbon in Siberian-Arctic shelf waters, J. Geophys. Res. - Oceans, 119, 1-12, doi: 10.1002/2014JC010261, 2014.

Wanninkhof, R.: Relationship between wind speed and gas exchange over the ocean, J. Geophys. Res., 97, 7373–7382, 1992.

Wanninkhof, R. and McGillis, W. R.: A cubic relationship between air-sea CO_2 exchange and wind speed, Geophys. Res. Lett., 26, 1889–1892, 1999.

Weiss, R. F.: Carbon dioxide in water and seawater: the solubility of a non-ideal gas, Mar. Chem., 2, 203-215, 1974.

Wood, K. R., Bond, N. A., Danielson, S. L., Overland, J. E., Salo, S. A., Stabeno, P. J., and Whitefield, J.: A decade of environmental change in the Pacific Arctic region, Prog. Oceanogr., 136, 12–31, 2015.

Yakushev, E.V. and Sørensen, K.: On seasonal changes of the carbonate system in the Barents Sea: observations and modeling, Marine Biology Research, 9 (9), 822-830, http://dx.doi.org/10.1080/17451000.2013.775454, 2013.

Zatsepin, A. G., Morozov, E. G., Paka, V. T., Demidov, A. N., Kondrashov, A. A., Korzh, A. O., Kremenetskiy V. V., Poyarkov, S. G., and Soloviev, D. M.: Circulation in the Southwestern Part of the Kara Sea in September 2007, Oceanology, 50 (5), 643–656, 2010.

.

Table 1. Mean values and standard deviations for ΔpCO_2 (µatm), hourly averaged wind speed (U_{hourly}), and air-sea CO_2 fluxes (F_{CO2}) in the study area in 2006, 2007, and 2009*.

	ΔpCO_2, µatm			U_{hourly}, m sec^{-1}			F_{CO2},** mmol m^{-2} day^{-1}		
	2006	2007	2009	2006	2007	2009	2006	2007	2009
Barents Sea	**-184±25** (-211 ÷ -146) *n = 9*	**-94±30** (-153 ÷ -12) *n = 345*	**-215±31** (-246 ÷-156) *n = 13*	**3.8±1.8** (0.8-7.8)	**9.0±3.8** (1.4-17.6)	**4.2±2.1** (2-9)	**-3.2±6.1** (-19.3 ÷ 0.0)	**-27.9±31.8** (-160.9 ÷ -0.1)	**-0.6±0.4** (-1.1 ÷ 0.0)
Kara Sea	**-114±13.8** (-123÷−104) *n = 2*	**-46±21** (-94 ÷ -1) *n = 303*	**-179±36** (-221÷-109) *n = 19*	**9.9±4.2** (6.9 – 12.8)	**14.3±4.6** (1.5-21.7)	**8.4±2.6** (2.5-13.6)	**-32.8±31.8** (-55.3÷−10.3)	**-50.7±42.1** (-170.0 ÷ 0.0)	**-18.3±19.4** (-71.0 ÷ 0.0)
Laptev Sea	**-95±50** (-182 ÷ -2) *n = 15*	**-22±40** (-120 ÷ 82) *n = 556*	**-101±40** (-145÷ -42) *n = 16*	**4.7±2.4** (0.4-11.0)	**5.0±2.3** (0.6-12.1)	**6.2±4.6** (1.0-16.2)	**-4.2±6.4** (-17.8 ÷ 0.0)	**-0.8±2.1** (-16.1 ÷ 6.7)	**-15.7±34.5** (-136.2 ÷0.0)
East Siberian Sea	**-107±12** (-117 ÷ -93) *n = 3*	**-4±11** (-63 ÷ 20) *n = 587*	**-89±6** (-101÷ -83) *n = 6*	**7.5±3.9** (3.3-11.1)	**7.6±3.3** (0.4-13.1)	**1.6±0.8** (0.9-2.9)	**-5.8±5.5** (-11.6 ÷ 0.8)	**0.2±2.2** (-15.0 ÷ 9.2)	**-0.03±0.0** (-0.1 ÷ 0.0)

*Maximum variability of each parameter is shown in parentheses; the number of measurements (n) is shown in italics.

**Flux calculated according to Wanninkhof and McGillis (1999); negative values correspond to CO_2 flux into the ocean.

(a)

(b)
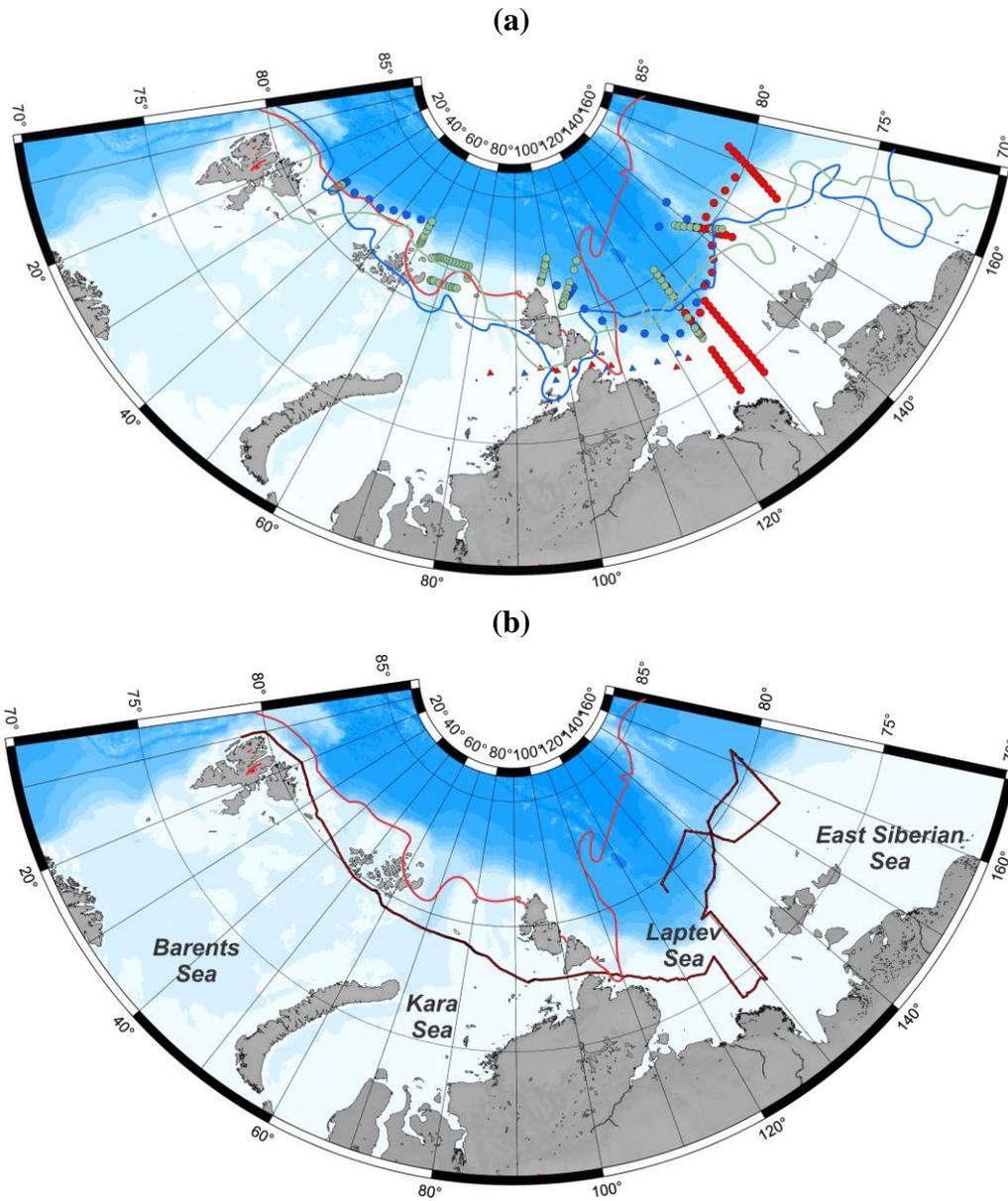
Figure 1: Ship routes and positions of oceanographic stations in the study area. (a) Positions of oceanographic stations performed in 2006, 2007, and 2009 are marked as colored circles: 2006 - blue; 2007 – red; 2009 – green. Position of the sea-ice edge during the expeditions is marked as colored curved lines: 2006 - blue; 2007 - red; 2009 - green; (b) the ship's route, along which the high-frequency measurements were performed in 2007.

(a)   **(b)**
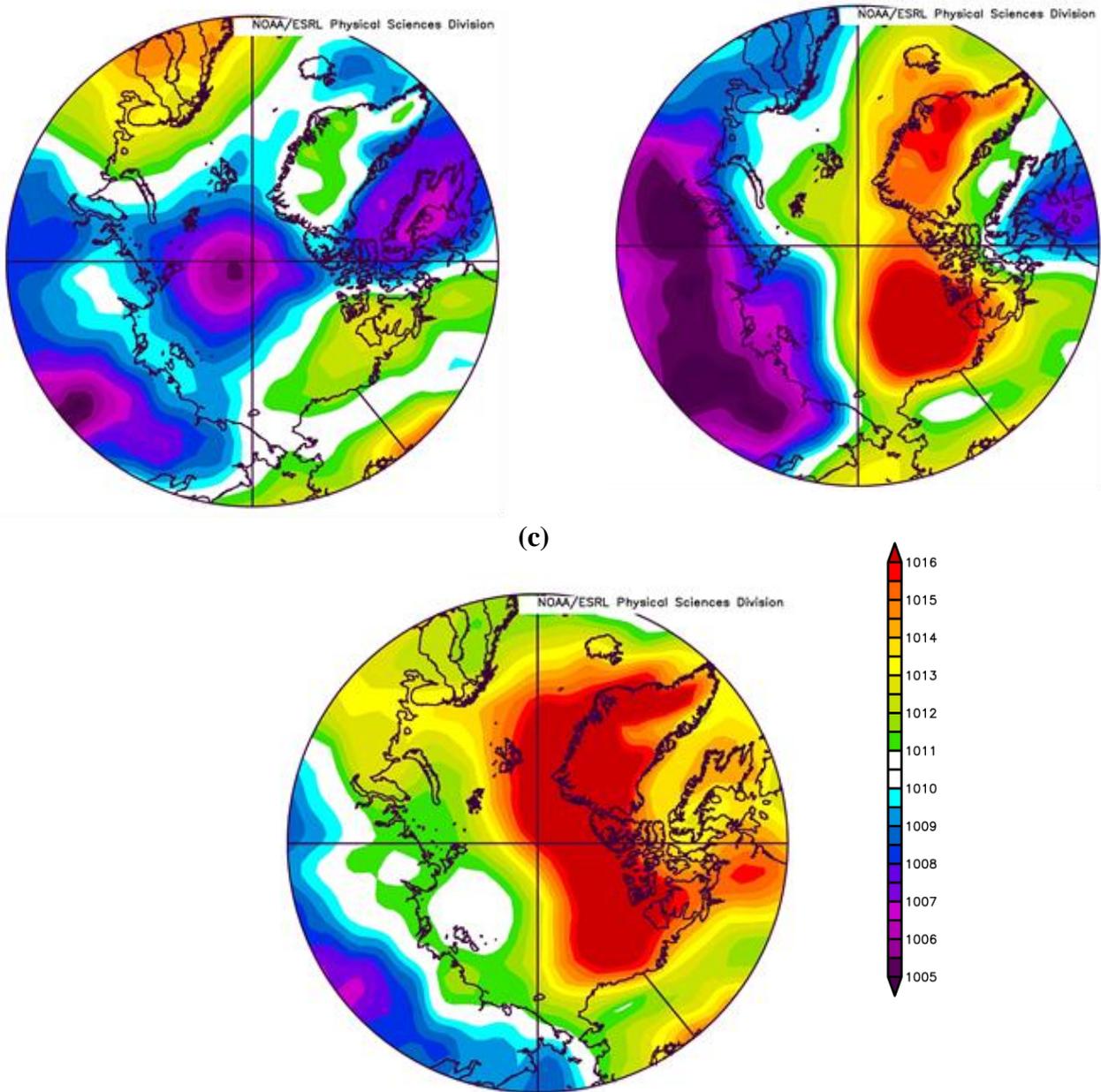
(c)

Figure 2: SLP fields (mbar) averaged over the summer season of 2006 (a), 2007 (b), and 2009 (c) from National Centers for Environmental Prediction (NCEP) data (www. esrl.noaa.gov).
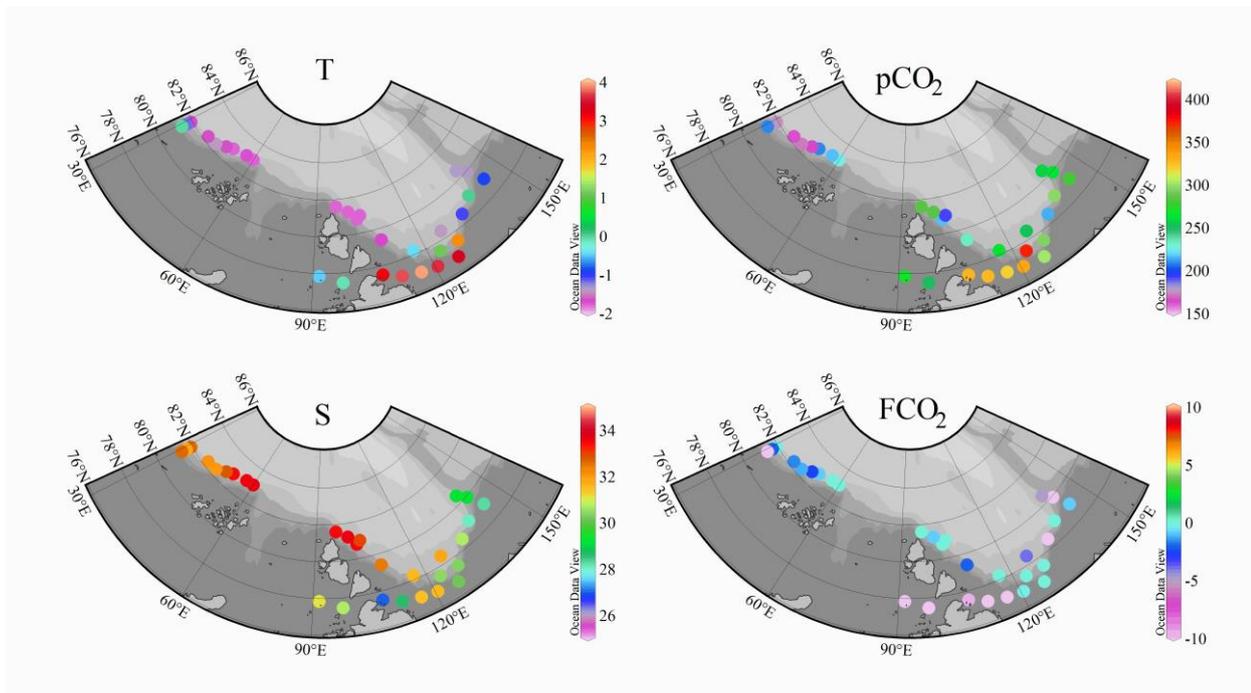
**Figure 3: Spatial distribution of sea surface temperature (T, °C), salinity (S), pCO₂ (μatm), and air-sea CO₂ fluxes (F_CO2, mmol m⁻²
day⁻¹) during the 2006 study.**
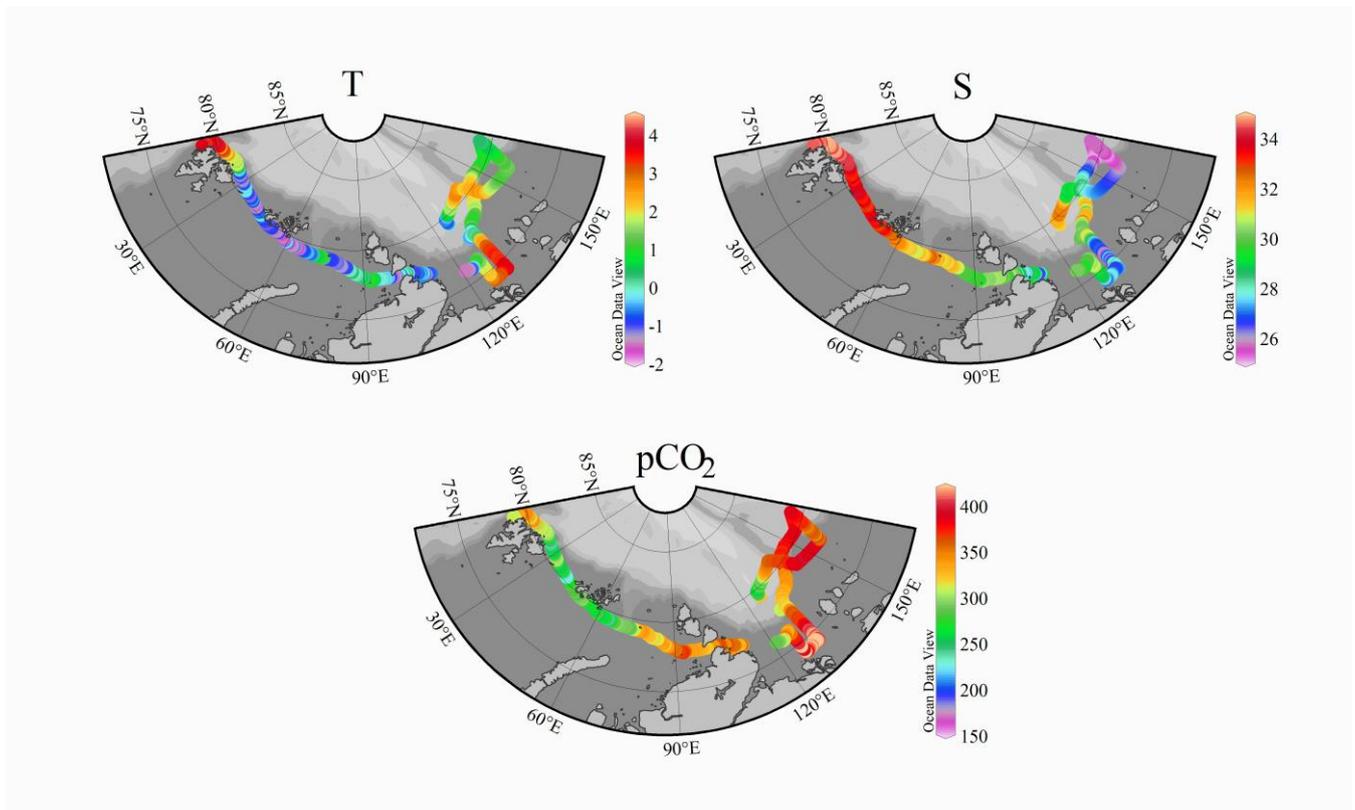
Figure 4: Spatial distribution of sea surface temperature (T, °C), salinity (S), and pCO₂ (µatm) during the 2007 study.
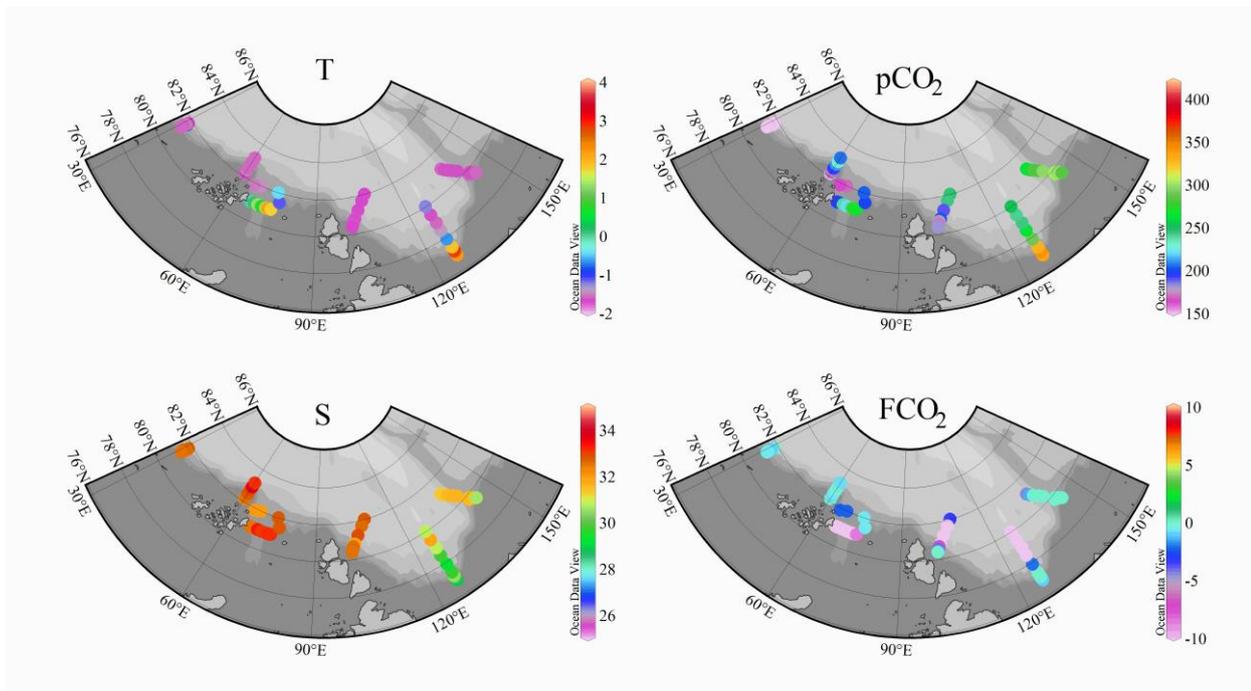
**Figure 5: Spatial distribution of sea surface temperature (T, °C), salinity (S), pCO₂ (μatm), and air-sea CO₂ fluxes (F_CO2, mmol m⁻²
day⁻¹) during the 2009 study.**
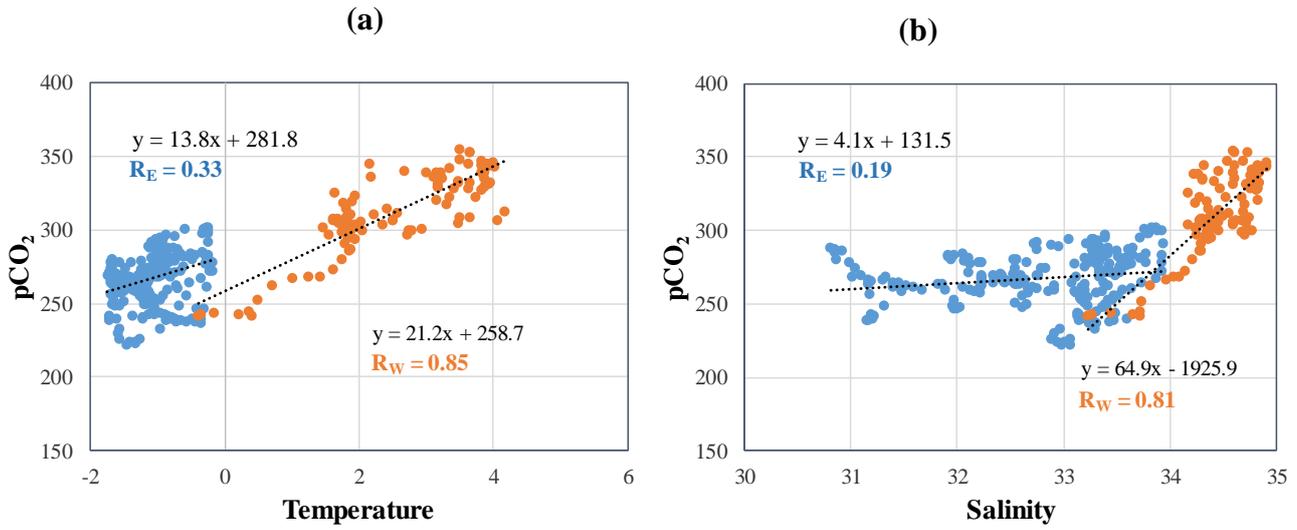
Figure 6: Relationship between pCO₂ (µatm) and temperature (°C) (a), and between pCO₂ and salinity (b) in the northern Barents Sea: western part – W, orange color, eastern part – E, blue color.
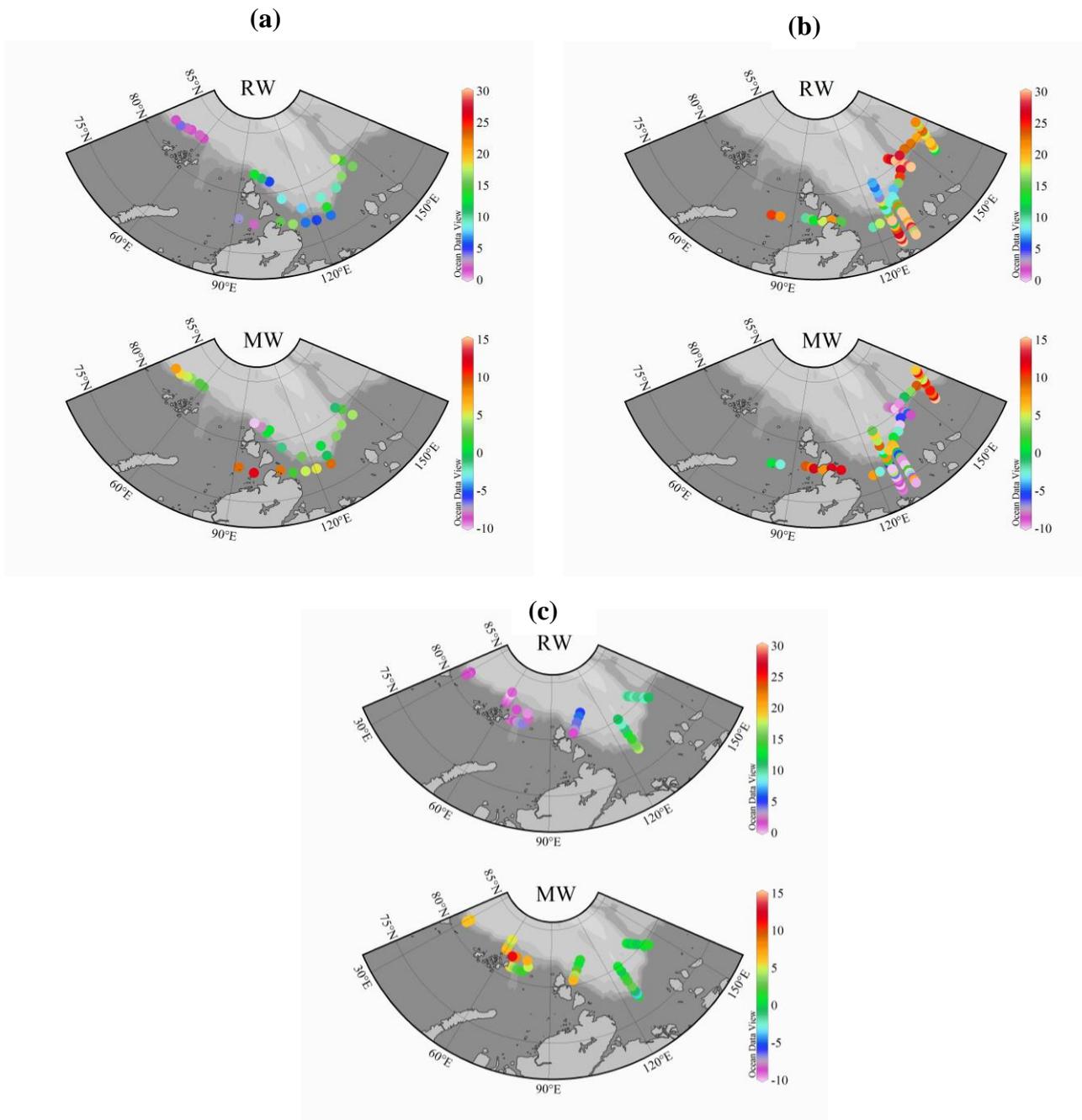
Figure 7: Spatial distribution of fractions of RW (%) and sea ice MW (%) in surface water during the 2006 (a), 2007 (b), and 2009 (c) studies.
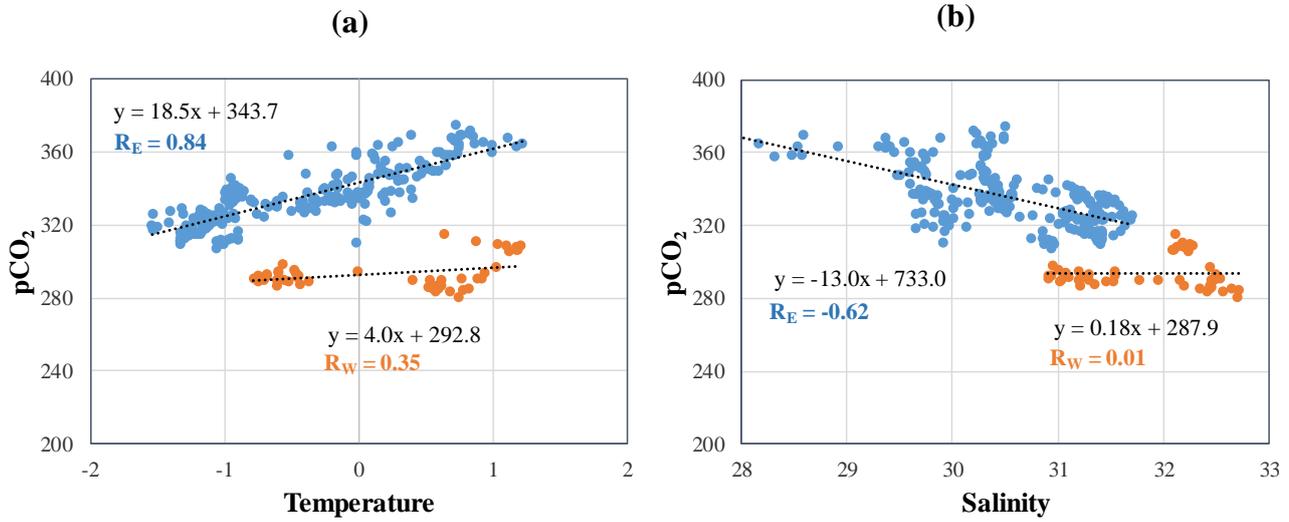
Figure 8: Relationship between pCO₂ (µatm) and temperature (°C) (a), and between pCO₂ and salinity (b) for samples collected in the western (W, orange color) and eastern (E, blue color) Kara Sea during the 2007 study.
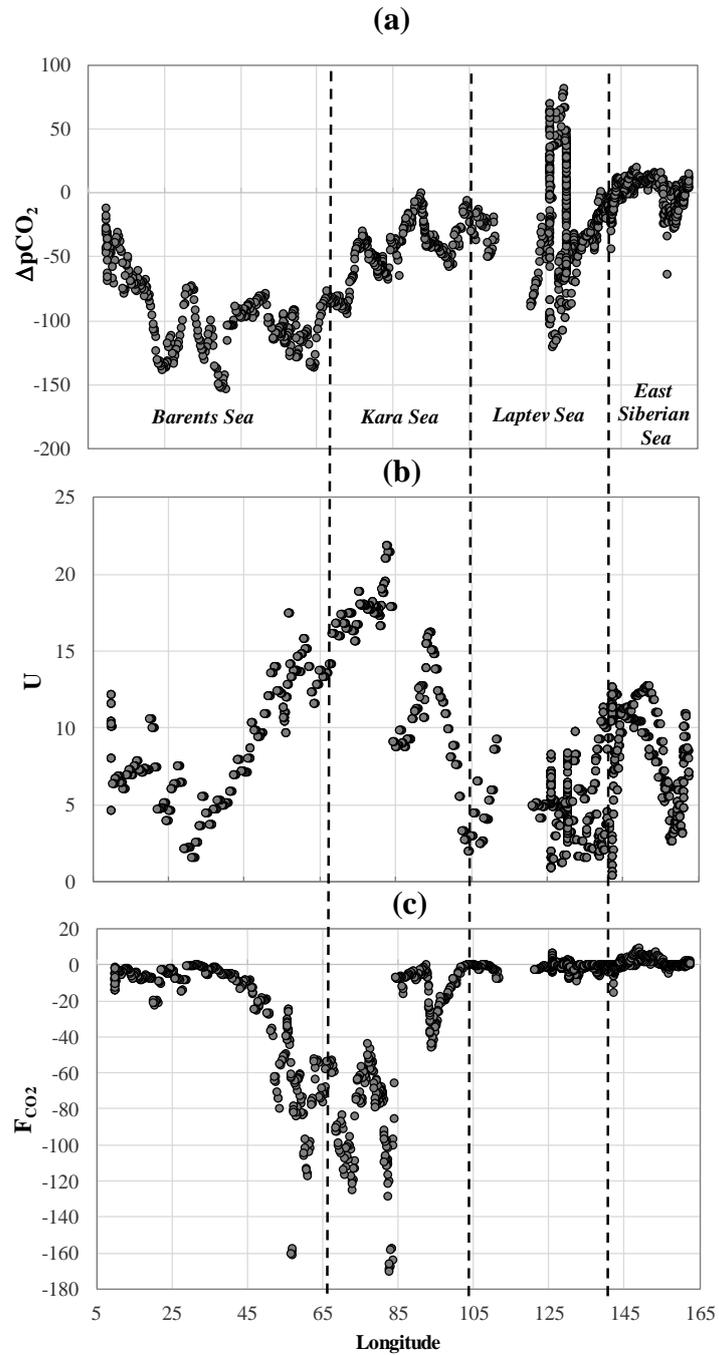
Figure 9: Distribution of (a) ΔpCO_2 (µatm), (b) wind speed (U, m s^{-1}), and (c) air-sea CO$_2$ fluxes (F$_{CO2}$, mmol m^{-2} day^{-1}) along the ship's route in 2007.
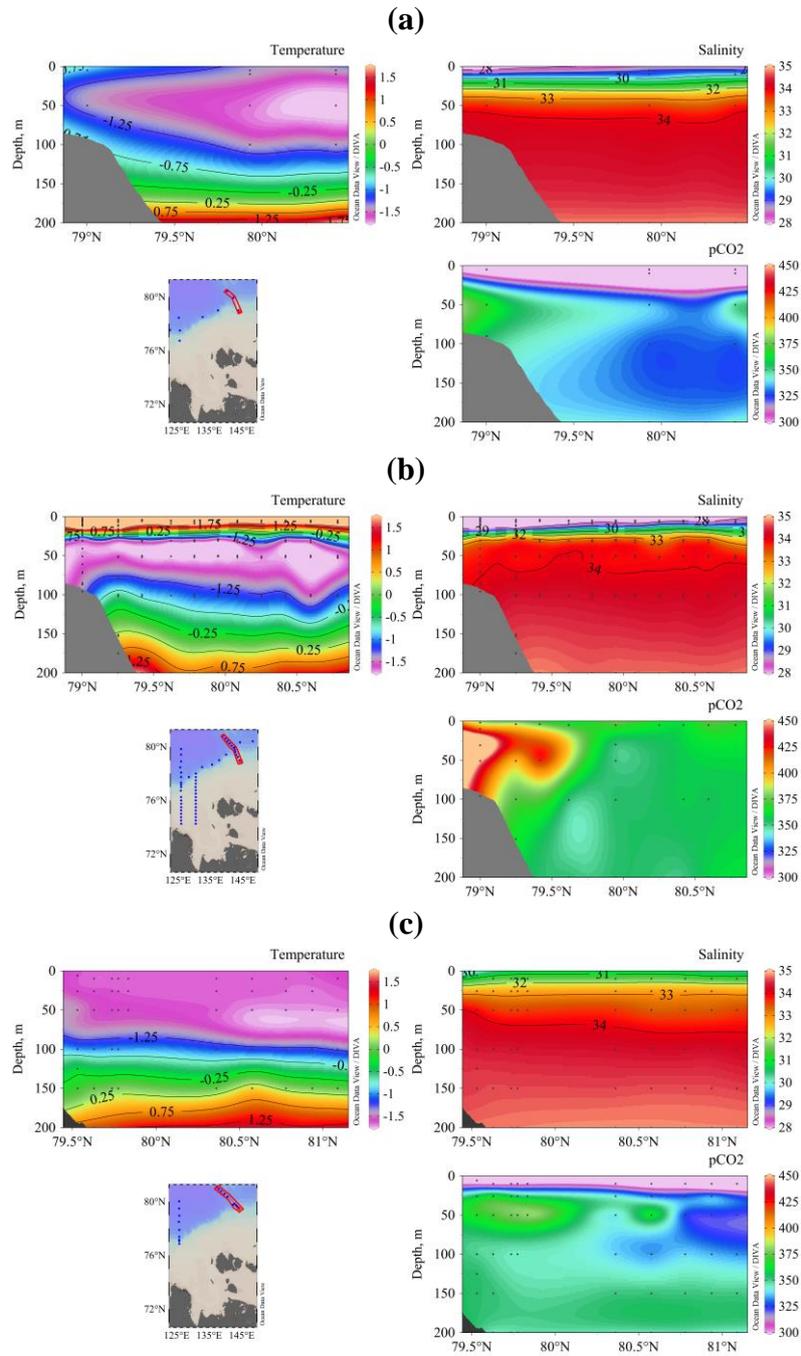
Figure 10: Distribution of temperature (°C), salinity, and pCO₂ (µatm) along the transect across the continental slope of the New Siberian Islands at ~140-145° E during the 2006 (a), 2007 (b), and 2009 (c) studies.
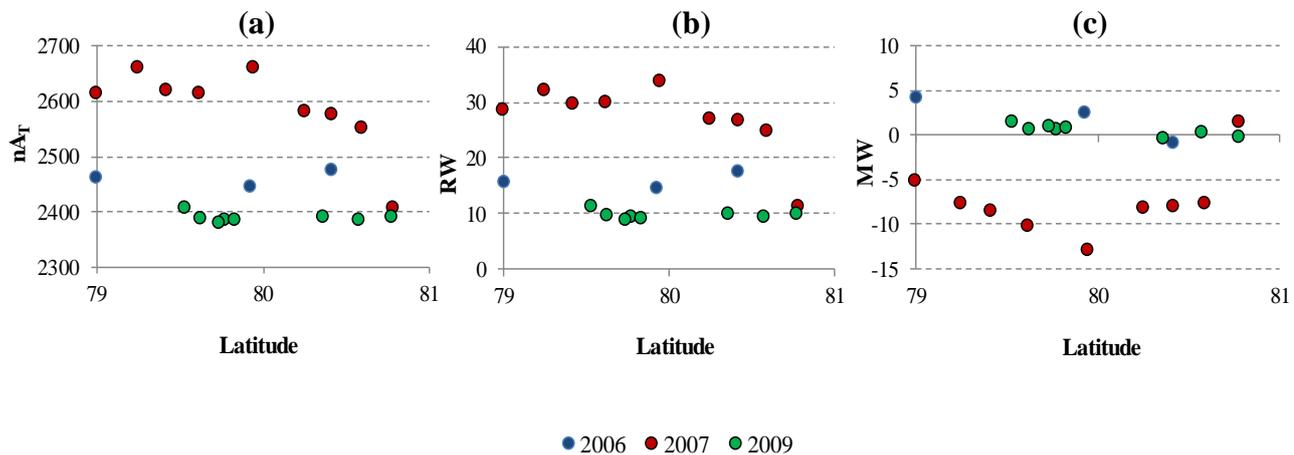
Figure 11: Distribution of (a) surface normalized A_T (nA_T, µmol kg^{-1}) and fractions (b) of RW (%) and (c) sea ice MW (%) along the transect across the continental margin of the New Siberian Islands at ~140-145° E in 2006, 2007, and 2009.